

PNNL-32743

Machine Learning Software for Cylindrical Battery Design and Performance Prediction

March 2022

Bingbin Wu
Jun Lu
Dianying Liu
Huifeng Zhou
Jason Hou
Daniel Deng
Jie Xiao

DISCLAIMER

This report was prepared as an account of work sponsored by an agency of the United States Government. Neither the United States Government nor any agency thereof, nor Battelle Memorial Institute, nor any of their employees, **makes any warranty, express or implied, or assumes any legal liability or responsibility for the accuracy, completeness, or usefulness of any information, apparatus, product, or process disclosed, or represents that its use would not infringe privately owned rights.** Reference herein to any specific commercial product, process, or service by trade name, trademark, manufacturer, or otherwise does not necessarily constitute or imply its endorsement, recommendation, or favoring by the United States Government or any agency thereof, or Battelle Memorial Institute. The views and opinions of authors expressed herein do not necessarily state or reflect those of the United States Government or any agency thereof.

PACIFIC NORTHWEST NATIONAL LABORATORY
operated by
BATTELLE
for the
UNITED STATES DEPARTMENT OF ENERGY
under Contract DE-AC05-76RL01830

Printed in the United States of America

Available to DOE and DOE contractors from
the Office of Scientific and Technical
Information,
P.O. Box 62, Oak Ridge, TN 37831-0062
www.osti.gov
ph: (865) 576-8401
fox: (865) 576-5728
email: reports@osti.gov

Available to the public from the National Technical Information Service
5301 Shawnee Rd., Alexandria, VA 22312
ph: (800) 553-NTIS (6847)
or (703) 605-6000
email: info@ntis.gov
Online ordering: <http://www.ntis.gov>

Machine Learning Software for Cylindrical Battery Design and Performance Prediction

March 2022

Bingbin Wu
Jun Lu
Dianying Liu
Huifeng Zhou
Jason Hou
Daniel Deng
Jie Xiao

Prepared for
the U.S. Department of Energy
under Contract DE-AC05-76RL01830

Pacific Northwest National Laboratory
Richland, Washington 99354

Abstract

A software that delivers optimal design parameters and performance predictions for cylindrical cells, which can range in size from micro batteries to EV batteries, is developed. The Cylindrical battery design V1.0 is comprised of three types of cylindrical batteries, Micro battery (Primary), Micro battery (Secondary) and 18650/21700/xxxxx cylindrical battery. The software was developed in MATLAB. The software has the capability to output the cell design with the capacity ranges from several mAh to several million Ah. The software utilizes machine learning and includes a graphical user interface to enable rapid prototyping to accelerate energy storage research, development, and manufacturing.

Acknowledgments

The research described in this report was conducted under the Laboratory Directed Research and Development (LDRD) Program as a strategic investment at the Pacific Northwest National Laboratory (PNNL), a multiprogram national laboratory operated by Battelle for the U.S. Department of Energy. PNNL is a multi-program national laboratory operated for the U.S. Department of Energy (DOE) by Battelle Memorial Institute under Contract No. DE-AC05-76RL01830.

Contents

Abstract.....	ii
Acknowledgments.....	iii
1.0 Introduction	1
2.0 Method, Discussion, and Results.....	2
2.1 Machine learning software development for cylindrical Li/CFx primary micro battery	2
2.1.1. Data collection with Li/CFx micro batteries	4
2.1.2. Machine learning process and prediction on the key parameters in Li/CFx primary micro battery.....	7
2.1.3. Software development and verification.....	14
2.2 Software development for cylindrical 18650/21700/xxxxx lithium-ion battery.....	20
2.2.1. Cell disassembly and data collected with commercial cylindrical LIBs.....	20
2.2.2. Software development.....	24
2.3 Summary	29
3.0 References.....	30

1.0 Introduction

Cylindrical batteries are the most common cell type in use today. They offer high energy density, good dimension stability, and reliability through the manufacturing process. They have been used to power miniature sensors, small consumer electronic devices, and large battery packs fueling electric vehicles that reduce greenhouse gas emissions.¹ Designing a cylindrical battery is more complicated than a pouch cell due to the wound structure and the different material loadings in one electrode, making it difficult for researchers and organizations to quickly assess their innovations in realistic batteries. A convenient tool such as the software proposed in this project is urgently needed to accelerate research innovation and domestic battery manufacturing.

Rational design of practically usable batteries must consider not only the electrical performance (energy density, impedance) but also battery dimensions and space utilization, cycling performance, cost reduction, and device manufacturability. All these factors make cell design a complex, error-prone, and time-consuming task. The proposed software embedded with machine-learning algorithms will address these considerations to simplify the process.

Recently, PNNL has released analogous software for Li-metal pouch cell design (see Fig. 1) supported by the Battery 500 Consortium.² In this work, we will leverage our battery design experience and machine-learning expertise to develop software specifically for cylindrical primary batteries based on chemistries from primary and secondary lithium metal batteries as well as lithium-ion batteries. Another important application of cylindrical batteries is the micro batteries for wearable electronics, downsized sensors, and implantable devices.^{3,4}

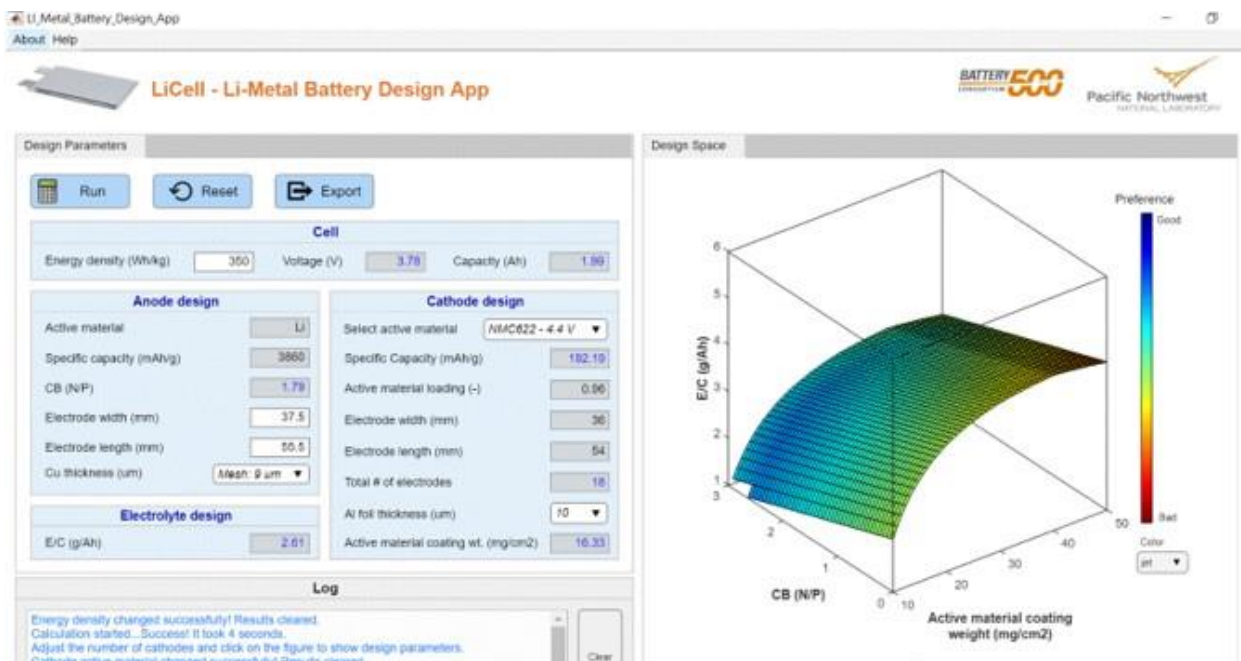


Figure 1. Software for Li metal pouch cell design by batt500.

2.0 Method, Discussion, and Results

2.1 Machine learning software development for cylindrical Li/CFx primary micro battery

Fig.2 shows the workflow of the software for cylindrical Li/CFx micro battery. First, the user inputs the requirements of the micro battery in the software, then the software automatically analyzes the inputted parameters and determines the battery type required, energy type or power type, through supervised learning. After that, the software performs the cell design according to the learned results and finally exports the detailed cell design information and estimated performances. However, how is the software built?

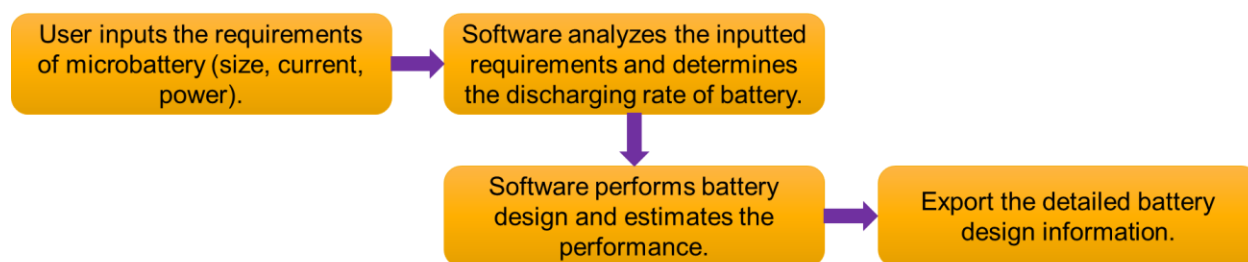


Figure 2. Workflow chart of cylindrical micro battery design software.

Over the past eight years, the cylindrical micro battery with the Li/CFx chemistry has been studied and produced extensively at PNNL. As shown in Fig.3, the jellyroll is produced by a winding process with alternative cathode sheet, separator sheet and anode sheet. Here, we focus on the Li/CFx micro battery as this chemistry has very high energy density and low self-discharge rate. The CFx cathode active material will be mixed with binder and carbon additive to produce the cathode electrode. Thin Li metal foil will be used as anode electrode directly. The software development is also based on this chemistry. The areal loading, percentage, pressing density of CFx cathode electrode, and its size will affect the energy and power of the micro battery. Figuring out the relationships between these key factors and cell performances is crucial to develop the software.

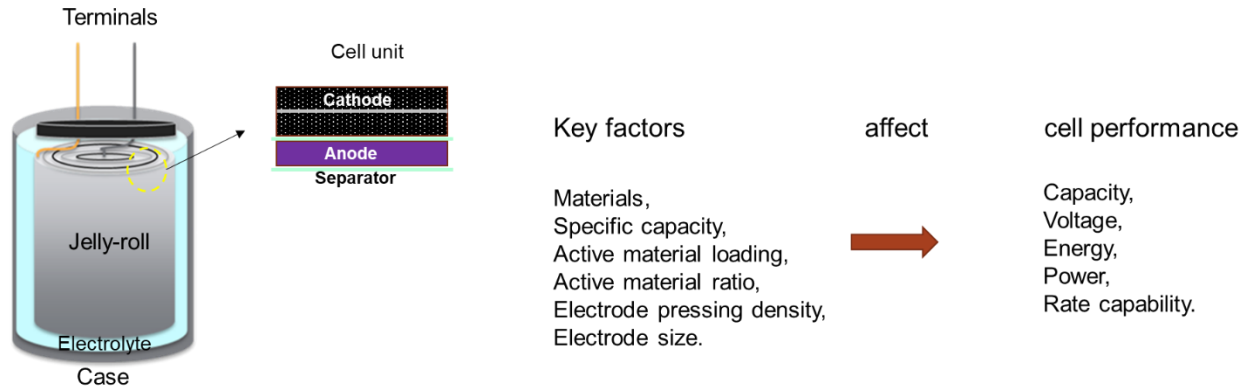


Figure 3. Schematic of cylindrical micro battery and its relevant key factors and cell performances.

In order to bridge the key factors and cell performances in Fig.3, five different sizes of micro battery with different CFx ratio, loading (or areal coating weight) will be produced and tested under four different discharge rates (Fig.4). Note that 'MBxxxxx' is used to describe the micro battery (MB) model, where the first two digitals after 'MB' represent the diameter of micro battery and the rest represent the height of the micro battery. In this work, we choose MB1820, MB1830, MB1842, MB3060 and MB47149 as our battery objects, the volume of these batteries ranges from 5 mm³ to 300 mm³. MB1842, MB3060 and MB47149 are the universal models we have worked on for so many years and we have plenty of experiences to produce them. To the best of our knowledge, MB1820 with volume of 5 mm³ is the smallest cylindrical battery in the world. That being said, we will have enhanced capability to produce smaller micro battery after this project. After collecting the data, we will analyze the relationships between the electrode parameters and cell performance, bridging them with equations. Also, a random forest supervised machine learning model will be introduced to do classification work for the micro battery. With these relationships and equations, a preliminary cell design program will be developed in EXCEL first and then transferred to a programmer for further software development in MATLAB.

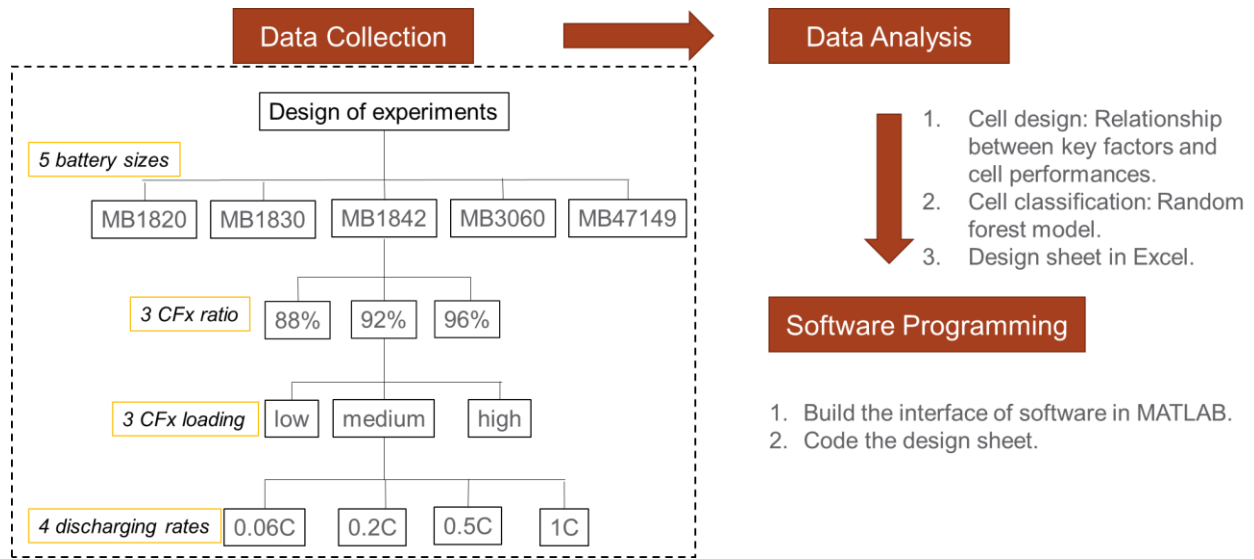
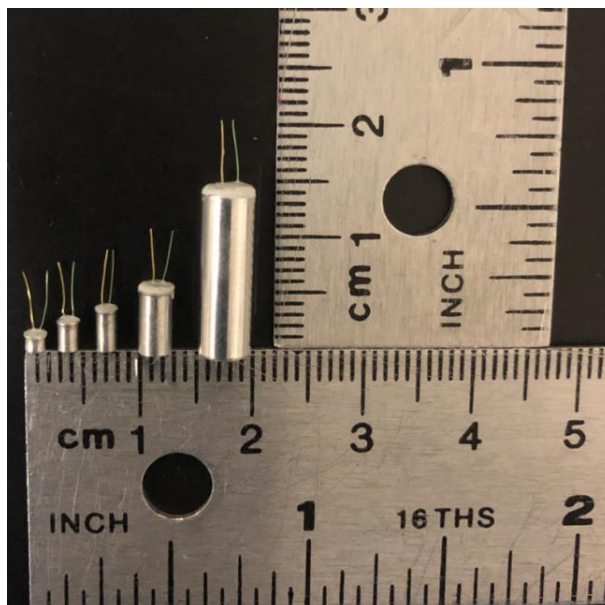


Figure 4. Method to build the software for cylindrical micro battery.

2.1.1. Data collection with Li/CFx micro batteries

According to Fig.4, at least twelve micro batteries have been produced for each size with different CFx ratio and loading (Fig.5). After production, the micro batteries will be discharged at four different discharging rates, 0.06C, 0.2C, 0.5C and 1C. A C-rate is a measure of the rate at which a battery is discharged relative to its maximum capacity. A 1C rate means that the discharge current will discharge the entire battery in 1 hour. The capacity, specific capacity, energy density, working voltage, driving voltage, gravimetric energy density and parameters for supervised random forest learning model at different discharging rate are collected (Fig.6). All the data analysis and software calculations are reliant on this data.



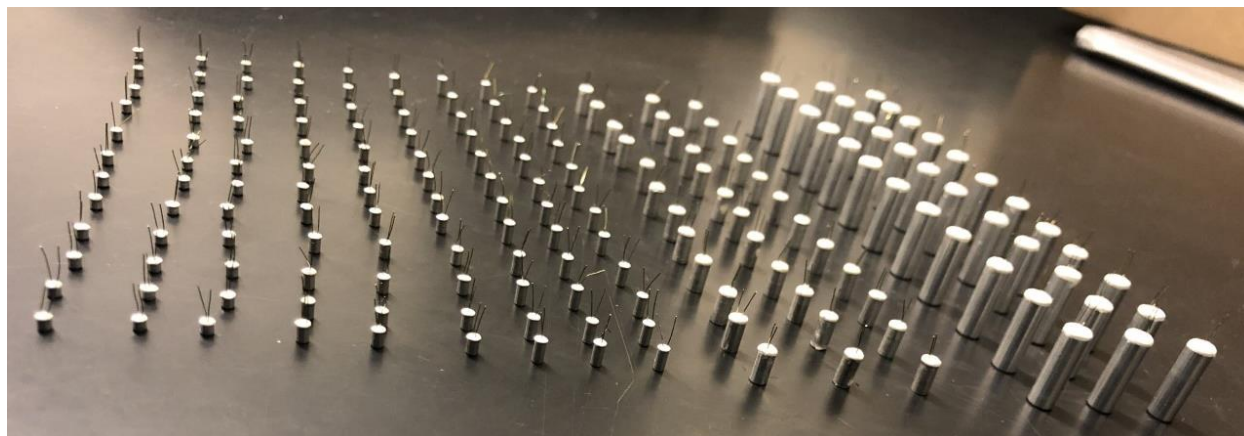


Figure 5. The digital photos of five different sizes of Li/CFx micro batteries (top) and production of these batteries with different CFx ratio and loading (bottom).

diameter	model	loading	Coating weight (mg/cm)	Thickness, um	Press density, c	0.06 C Capacity (nr)	0.2C capacity (mA)	0.5C capacity	1C capacity (nr)	0.06C Specific	0.2C specific	0.2C Capacity	0.5C specific	0.5C Capacity	1C specific ca	1C capacity re
18 series	1842	88%	19.1	130.6	1.65	1.6	1.44	1.32	1.03	748	657.00	0.88	602.00	0.80	499.00	0.67
		88%	27.6	174.5	1.73	1.57	1.38	1.04	0.86	723	658.00	0.91	459.00	0.63	373.00	0.52
		88%	33.5	206.2	1.75	1.63	1.34	0.67	0.56	716	622.00	0.87	295.00	0.41	246.00	0.34
		32%	18.7	132.3	1.59	1.54	1.30	1.18	0.86	683	580.00	0.85	517.00	0.76	368.00	0.54
		32%	29.3	190.6	1.62	1.61	1.30	0.88	0.54	707	553.00	0.78	378.00	0.53	223.00	0.32
	32%	33.2	218.1	1.64	1.71	1.27	0.78	0.50	709.00	503.00	0.71	310.00	0.44	163.50	0.26	
		96%	19.2	126.3	1.63	1.5	1.42	1.29	1.04	632.00	665.00	0.96	678.00	0.89	480.00	0.63
		96%	27.9	175.7	1.73	1.67	1.47	1.07	0.56	655.00	618.00	0.94	443.00	0.68	220.00	0.34
		96%	32.8	201.9	1.76	1.53	1.22	1.08	0.36	604.00	524.00	0.87	444.00	0.74	144.00	0.24
		model	loading	Coating weight (mg/cm)	Thickness, um	Press density, c	0.06 C Capacity (nr)	0.2C capacity (mA)	0.5C capacity	1C capacity (nr)	0.06C Specific	0.2C specific	0.2C Capacity	0.5C specific	0.5C Capacity	1C specific ca
	1830	88%	22.4	148.3	1.68	1.07	0.98	0.76	0.58	757.00	672.00	0.89	546.00	0.72	400.00	0.53
		88%	32.6	193.8	1.82	1.09	0.87	0.72	0.51	633.00	498.00	0.79	407.00	0.64	285.00	0.45
		88%	40.1	223.6	1.92	1.06	0.60	0.50	0.19	719.00	390.00	0.54	318.00	0.44	117.00	0.16
		32%	22.6	146.7	1.71	1.05	0.81	0.75	0.66	688.00	585.00	0.85	528.00	0.77	453.00	0.66
		32%	27.6	178	1.69	1.1	0.94	0.84	0.66	648.00	627.00	0.97	573.00	0.88	421.00	0.65
96%	36.8	224	1.76	0.98	0.95	0.65	0.40	560.00	498.00	0.89	357.00	0.64	246.00	0.44		
	21.6	153.7	1.56	0.324	0.89	0.72	0.60	658.00	584.00	0.89	531.00	0.81	424.00	0.64		
	96%	31	185.1	1.82	1.11	0.86	0.60	x[can't work]	663.00	498.00	0.75	375.00	0.57	#VALUE!		
	96%	36.1	210.9	1.84	1.25	0.88	0.72	x[can't work]	670.00	530.00	0.79	370.00	0.55	#VALUE!		
	model	loading	Coating weight (mg/cm)	Thickness, um	Press density, c	0.06 C Capacity (nr)	0.2C capacity (mA)	0.5C capacity	1C capacity (nr)	0.06C Specific	0.2C specific	0.2C Capacity	0.5C specific	0.5C Capacity	1C specific ca	1C capacity re
1820	88%	22.4	148.3	1.68	0.52	0.48	0.48	0.37	714.00	672.00	0.94	617.00	0.86	494.00	0.63	
	88%	32.6	193.8	1.82	0.64	0.46	0.36	0.28	723.00	501.00	0.69	365.00	0.50	282.00	0.39	
	88%	40.1	223.6	1.92	0.65	0.38	0.24	0.11	753.00	466.00	0.62	322.00	0.43	143.00	0.19	
	32%	22.6	146.7	1.71	0.51	0.44	0.37	0.23	686.00	532.00	0.86	425.00	0.62	273.00	0.40	
	32%	27.6	178	1.69	0.54	0.4	0.31	0.21	686.00	514.00	0.75	380.00	0.55	293.00	0.43	
96%	36.8	224	1.76	0.6	0.35	0.30	0.16	695.00	410.00	0.59	343.00	0.49	228.00	0.33		
	23.8	153.7	1.56	0.6	0.498	0.38	0.23	663.00	591.00	0.88	369.00	0.59	321.00	0.48		
	96%	31	185.1	1.82	0.55	0.46	0.37	x[can't work]	627.00	518.00	0.83	421.00	0.67	#VALUE!		
	96%	33.8	185.9	1.99	0.495	0.413	0.35	x[can't work]	554.00	501.00	0.90	373.00	0.67	#VALUE!		
	model	loading	Coating weight (mg/cm)	Thickness, um	Press density, c	0.06 C Capacity (nr)	0.2C capacity (mA)	0.5C capacity	1C capacity (nr)	0.06C Specific	0.2C specific	0.2C Capacity	0.5C specific	0.5C Capacity	1C specific ca	1C capacity re
30 series	3060	88%	17	125.6	1.54	8.91	7.8	7.56	6.12	722.00	641.00	0.89	637.00	0.88	406.00	0.56
		88%	25.4	168.1	1.66	8.63	7.49	6.68	4.90	700.00	610.00	0.87	562.00	0.80	417.00	0.60
		88%	32.2	208.3	1.67	9.07	7.29	6.06	3.12	655.00	506.00	0.77	419.00	0.64	221.00	0.34
		32%	17.8	127.1	1.59	8.94	8.44	7.96	6.36	692.00	620.00	0.91	600.00	0.88	477.00	0.70
		32%	29.7	192.9	1.62	9.31	8.22	6.20	3.08	693.20	643.10	0.94	451.60	0.66	240.10	0.35
96%	32.7	233	1.68	9.23	8.33	6.18	2.84	635.00	561.00	0.88	458.00	0.72	192.00	0.30		
	96%	22.6	150.5	1.66	9.49	8.51	6.55	x[can't work]	683.00	613.00	0.90	469.00	0.69	#VALUE!		
	96%	28.2	188.8	1.62	9.12	8	6.72	x[can't work]	683.00	596.00	0.87	505.00	0.74	#VALUE!		
	96%	38.5	246.7	1.67	8.99	7.97	x[can't work]	x[can't work]	686.00	595.00	0.87	#VALUE!	#VALUE!			
	model	loading	Coating weight (mg/cm)	Thickness, um	Press density, c	0.06 C Capacity (nr)	0.2C capacity (mA)	0.5C capacity	1C capacity (nr)	0.06C Specific	0.2C specific	0.2C Capacity	0.5C specific	0.5C Capacity	1C specific ca	1C capacity re
47 series	47H9	88%	15.4	114.9	1.54	715	70.3	65.6	58.50	611.00	782.00	0.90	749.00	0.92	663.00	0.82
		88%	25.1	174.3	1.58	77	70.6	63.4	53.20	639.00	629.00	0.91	625.00	0.91	536.00	0.78
		88%	31.8	213.8	1.6	76.5	72.7	69.7	58.00	659.00	656.00	1.00	627.00	0.95	508.00	0.77
		32%	16.7	120.2	1.59	74.4	73.2	69.9	67.70	781.00	706.00	0.90	681.00	0.87	647.00	0.83
		32%	26.8	181.1	1.61	72.3	76.1	61.9	56.80	627.00	609.00	0.97	521.00	0.83	490.00	0.78
		32%	32.4	220.6	1.58	75.5	75	69.9	63.30	660.00	620.00	0.94	610.00	0.92	551.00	0.83
		96%	16	119.1	1.54	78.1	76.3	66.8	70.20	773.00	694.00	0.90	613.00	0.79	736.00	0.95
		96%	28.1	191.8	1.59	81.9	715	x[can't work]	x[can't work]	646.00	596.00	0.92	#VALUE!	#VALUE!	#VALUE!	
		96%	34.4	223.1	1.61	79.3	65.9	x[can't work]	x[can't work]	670.00	501.00	0.75	#VALUE!	#VALUE!	#VALUE!	
		model	loading	Coating weight (mg/cm)	Thickness, um	Press density, c	0.06 C Capacity (nr)	0.2C capacity (mA)	0.5C capacity	1C capacity (nr)	0.06C Specific	0.2C specific	0.2C Capacity	0.5C specific	0.5C Capacity	1C specific ca

Figure 6. Data sheet of five different sizes micro batteries with different CFx ratio and loading. The full data can be found in left Excel document.



data%20resource.xlsx

Electrodes/separator size determination

As mentioned above, the jelly roll of the micro battery is produced by a winding process. The size of the jelly roll depends on the size of cathode sheet, separator sheet and anode sheet. The size includes the width and length of each sheet. The width of electrodes/separator will affect the height of the jelly roll, while the length affects its diameter. The principle to determine the width of electrodes/separator is quite simple if we know the structure of micro battery. As showed in Fig.7, it's easy to determine the width of electrodes/separator as below:

Width of separator = Height of the battery - thickness of Torr seal - thickness of case (top and bottom) - thickness of rubber disk.

Width of the Li metal anode = Width of separator - Overhang of separator/Li metal.

Width of the CFx cathode = Width of Li metal anode - Overhang of Li/CFx electrode.

Overhang means the extra width of separator relative to Li metal anode or Li metal anode relative to CFx electrode. Large overhang would result in better safety in secondary battery and easy manufacture, but lower energy density. As we are working on primary battery and trying to increase the energy density, here, we will set 0.5 mm for overhang of the separator/Li metal anode and 0 mm for Li metal anode/CFx cathode.

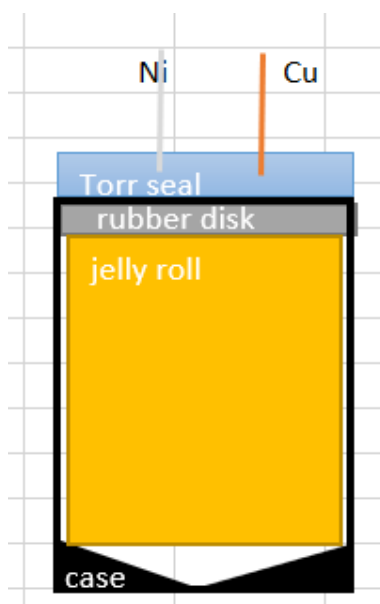
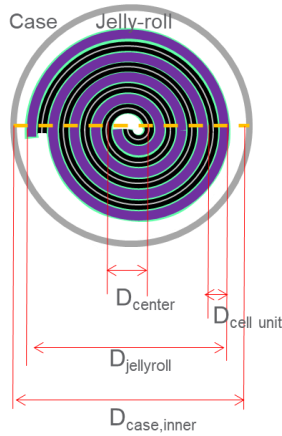


Figure 7. The sectional view of the structure of micro battery.

Determination of the length of electrodes/separator is a bit complicated. As shown in Fig.8, the diameter of the jelly roll is easier to determine if we know the diameter of the inner case and the gap degree. The gap degree is defined by equation (1) in Fig.8 and its value must be less than 1 so the jelly roll can be inserted into the case while leaving some room for jelly roll swelling and electrolyte. If the thickness of CFx electrode, Li metal electrode and separator are provided, then we will know how many loops are required for the jelly roll according to equation (2). The length of the CFx (n loops) or Li metal (n+1 loops) can then be calculated using equation (4),

the sum of arithmetic progression. The length of the separator can be achieved by doubling the length of Li metal anode with extra overhang.



Determine the length of electrodes and separator

$$(1) \text{ Gap degree} = \frac{D_{\text{jellyroll}}}{D_{\text{case, inner}}} \quad (\text{Gap degree should be less than 1 so the jellyroll can be inserted into case, usually around 0.9.})$$

$$(2) D_{\text{jellyroll}} = D_{\text{center}} + n * D_{\text{cell unit}} \quad (n \text{ is the numbers of semicircle of CFx electrodes.})$$

$$(3) D_{\text{cell unit}} = T_{\text{cathode}} + T_{\text{anode}} + 2 * T_{\text{separator}} \quad (T \text{ means thickness.})$$

$$(4) \text{ Length of CFx} = \frac{\pi}{2} * [D_{\text{center}} + D_{\text{cell unit}} + (D_{\text{center}} + 2 * D_{\text{cell unit}}) + \dots + (D_{\text{center}} + n * D_{\text{cell unit}})]$$

$$= \frac{\pi}{2} * (n * D_{\text{center}} + n * \frac{n-1}{2} * D_{\text{cell unit}})$$

Figure 8. The method to determine the length of electrodes.

2.1.2. Machine learning process and prediction on the key parameters in Li/CFx primary micro battery

Machine learning model used

Generalized linear model (GLM):

The general purpose of multiple regression is to quantify the relationship between several independent variables and a dependent variable. In general, the linear multiple regression can be estimated as:

$$Y = b_0 + \sum_{i=1}^k b_i * X_i \quad (1)$$

Regression Tree: Random forests (RF)

Random forests or random decision forests are an ensemble learning method for classification, regression and other tasks that operates by constructing a multitude of decision trees at training time and outputting the class that is the mode of the classes (classification) or mean prediction (regression) of the individual trees. Random decision forests correct for decision trees' habit of overfitting to their training set.

The prediction of RF model is obtained by a majority vote over the predictions of the individual trees. To specify a particular RF,

$$RF(x) = \text{sgn}(\sum_{i=1}^k RT_i(x)) \quad (2)$$

Data analysis

In this work, we built eight random forest models. The response variables are specific capacity and voltage. The explanatory variables include the height of a battery (mm), the volume of a battery (mm^3), loading, coating weight (mg/cm^2), the press density (g/cm^3), process parameter, charging rate, current (mA), mA/mm^3 , power (mW) and the mW/mm^3 .

All experimental observations

The experimental observations with retentions equal to or greater than 0.5 are selected to set up the machine learning problems. The total number of observations is 152, and they were split into training data and testing data. The training data contains 109 observations, and the testing data contains 43 observations.

The experimental observations under 0.06C

Charging a battery under ideal conditions is another major benchmark study, so we also study the relationship between response variables and the explanatory variables using a 0.06C charging rate. In this part, the training dataset has 31 observations, and the testing data has 14 observations.

Randoms forest model setups

The following table shows the details about those RF models. We predict the response variables such as specific capacity and voltage by using the explanatory variables from the battery design parameters.

Table 1. The explanation of RF models response variable and the explanatory variables

Response variable	Explanatory variables
Specific capacity under 0.06C	Height, diameter, coating weight, press density, process parameter
Voltage under 0.06C	Height, diameter, coating weight, press density, process parameter
Specific capacity	Height, diameter, volume, loading, coating weight, press density, process parameter
Specific capacity	Height, diameter, volume, loading, coating weight, press density, process parameter+current+ mA/mm^3
Specific capacity	Height, diameter, volume, loading, coating weight, press density, process parameter+power+ mW/mm^3
Voltage	Height, diameter, volume, loading, coating weight, press density, process parameter+current+ mA/mm^3
Voltage	Height, diameter, volume, loading, coating weight, press density, process parameter+power+ mW/mm^3
Voltage	Height, diameter, volume, loading, coating weight, press density, process parameter

PCA analysis

Figure 9 shows the PCA bi-plots, where the first two principal components are used to visualize the similarities among specific capacity or voltage and the input parameters. The first component accounted for 45.4%, and the second component accounted for about 24.6% of the total variance of specific capacity and input parameters (panel a). The first component accounted for 45.3%, and the second component accounted for about 19.5% of the total variance of voltage and input parameters (panel b). Panel a and b of Figure 9 both show the points with different colors for each of the rate conditions. Note that points close to each other correspond to observations with similar scores/projections onto the principal components. The ultra-low points are mixed in the region of the low group. And the bounty of high and ultra-high are not evident.

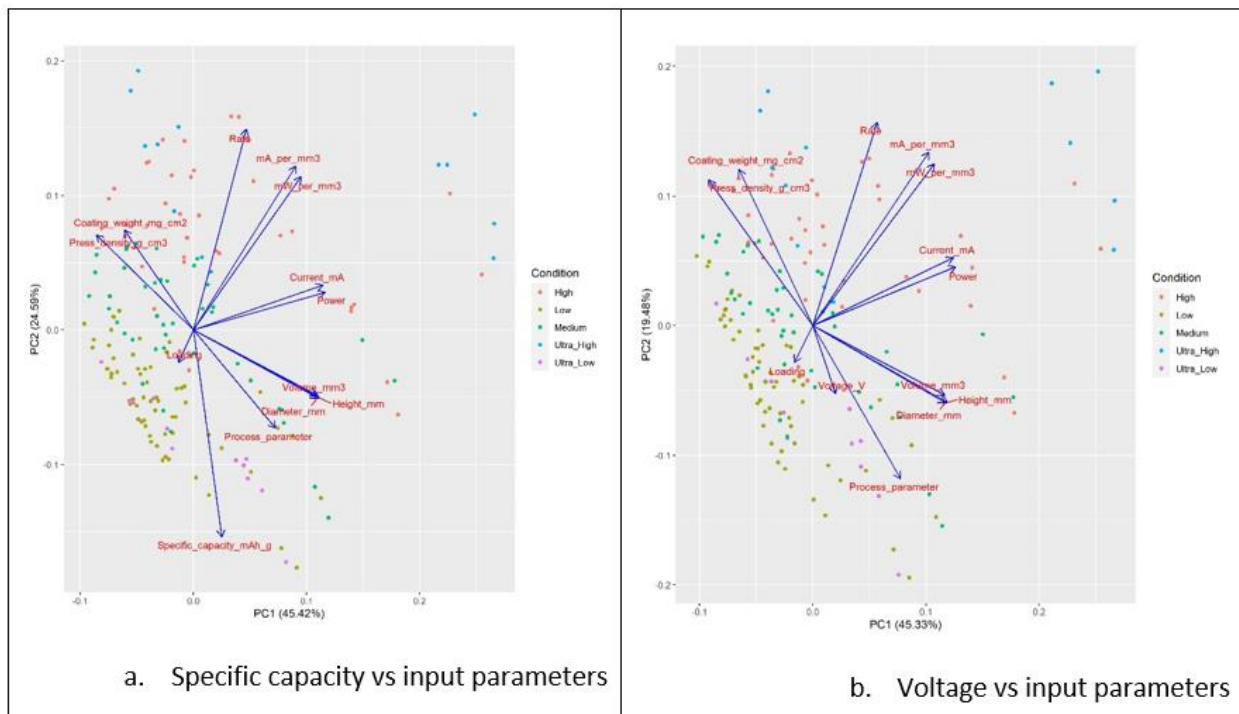


Figure 9. PCA biplot of among micro battery's input parameters and specific capacity and voltage

Feature importance

Specific capacity models

Figure 10 shows the feature importance of specific capacity RF models. Those three panels show that the rate is the dominant factor for the specific capacity RF models. The coating weight and the process parameter are comparable. Other parameters such as the height, diameter, and volume of a battery are not so that important. Current parameters and the power parameters are 4th and 5th most important, respectively.

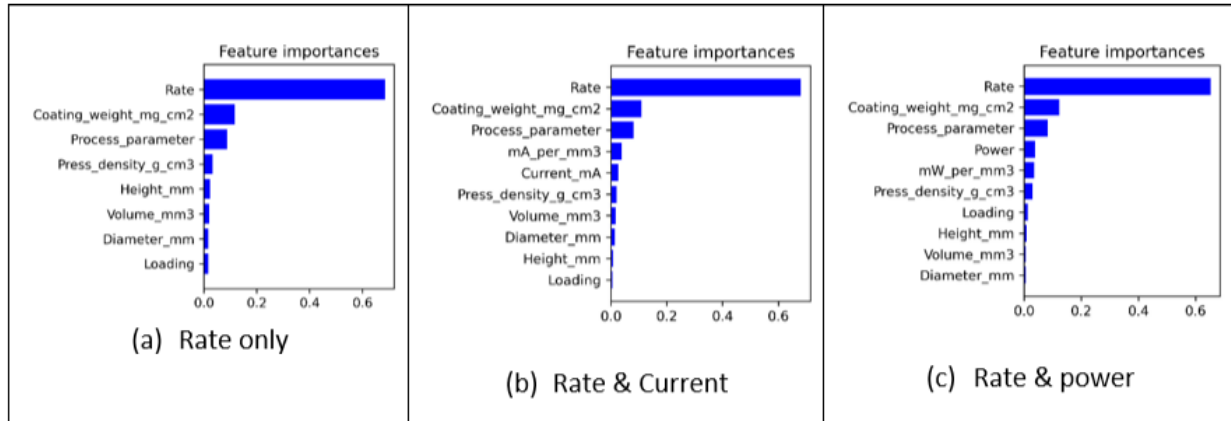


Figure 10. Feature importance of specific capacity models. Using (a) physical parameters and rate, (b) physical parameters, rate, and current variables, (c) physical parameters, rate, and power variables as explanatory variables.

Voltage models

Figure 11 shows the feature importance of voltage RF models. Those three panels show that the rate is the dominant factor for the voltage RF models. The importance of other parameters is weak and those parameter's feature importance are comparable.

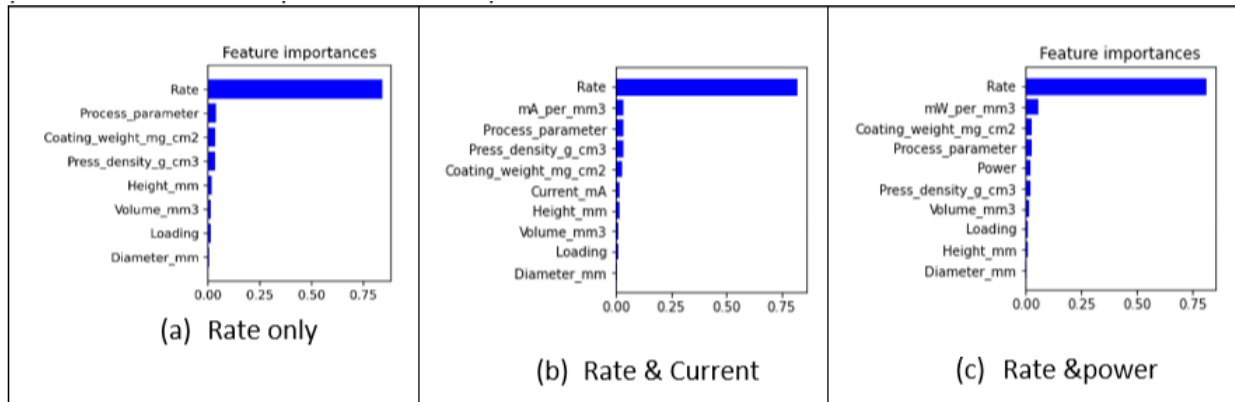


Figure 11. Feature importance of voltage models. Using (a) physical parameters and rate, (b) physical parameters, rate, and current variables, (c) physical parameters, rate, and power variables as explanatory variables.

Prediction Results

The predictions of RF models

Prediction of rate conditions

We use the current-based model to predict the rate conditions and use the micro battery's height, diameter, volume, current and current per volume as independent variables. We also

build a power-based model to predict the rate conditions too. The testing accuracy of the current-based model is 80%, and that of the power-based model is 76%. The two confusion matrixes show that most points are labeled correctly, but some are in the neighbor group. For the medium group, the current-based model is better than the power-based model. For the low group, the current-based model and the power-based model are comparable. Due to the small samples of ultra-high, ultra-low and high groups, it is hard to conclude.

Table 2. The confusion matrixes of different models for rate conditions

<pre> ==testing_Current_Training_Data_Splitted_verision== ===Confusion_Matrix_Current_Training_Data_Splitted_verision=== Ultra_High Ultra_High High Medium Low Ultra_Low Ultra_High 1 1 0 0 0 High 0 4 2 0 0 Medium 0 0 16 1 0 Low 0 0 1 17 1 Ultra_Low 0 0 0 4 2 </pre>						<pre> ==testing_Power_Training_Data_Splitted_verision== ===Confusion_Matrix_Power_Training_Data_Splitted_verision=== Ultra_High Ultra_High High Medium Low Ultra_Low Ultra_High 1 1 0 0 0 High 0 5 1 0 0 Medium 0 1 13 3 0 Low 0 0 1 17 1 Ultra_Low 0 0 0 4 2 </pre>					
---	--	--	--	--	--	---	--	--	--	--	--

Prediction of specific capacity

We compare the three methods' model of prediction of specific capacity. We consider the rate-based linear model as the native model. The GLM and RF models are applied. Figure 12 shows the predictions and prediction errors of different models. The y_Actual is the actual value of the experiment's specific capacity and is represented by black color from panel a. The blue points represent the prediction from RF models, and the green points represent the prediction of GLM models. The red ones are from the naïve model. In general, the naïve model's predictions have a small range. Most of the forecasts of RF models are close to actual values of specific capacity. Panel 2 shows the boxplot of absolute errors of the 7 models. The RF model's performance is the best; almost 75% of sample's predict errors are less than 10%, and nearly 95% of sample's predict errors are less than 20%. Some of the prediction errors of naïve models are very large, and almost 55% of samples' prediction errors are less than 10%. The overall ranges of predict errors of the GLM model are broader than that of RF models.

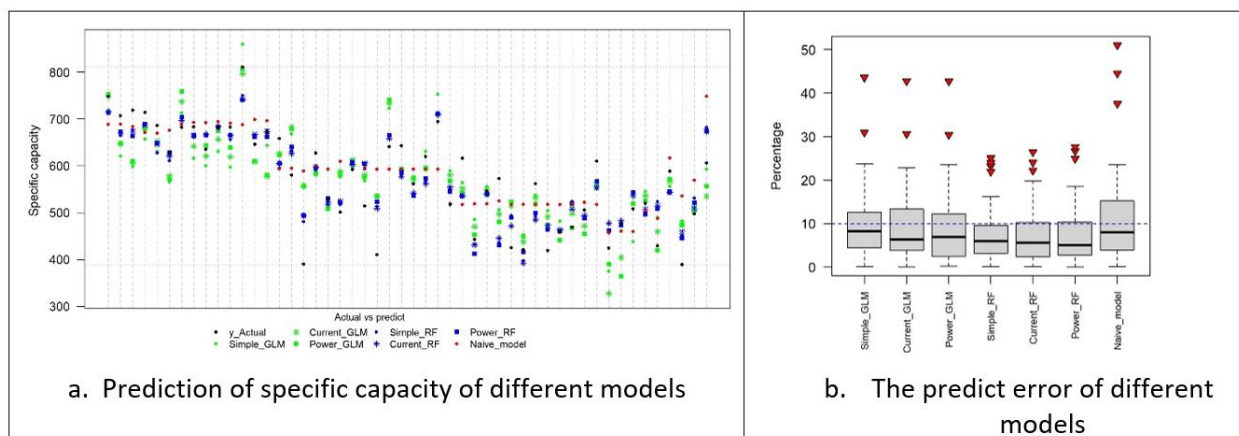


Figure 12. Specific capacity prediction scatter plot and the boxplot of predict absolute errors of different models

Prediction of voltage

We use the same method to predict the voltage. The naïve model of voltage prediction is the piecewise function. From panel a of Figure 13, the naïve model prediction has slight variation in each piece under the same range of the rate. For the actual voltage, naïve model has better forecasts than other models. The boxplot in panel b shows that the predicted errors of GLM and RF models are comparable. All 6 models can't handle the lower voltage prediction, and we may need more parameters and samples to study the voltage. The absolute errors' boxplot of the naïve model shows the significant variation between predictions of actual values.

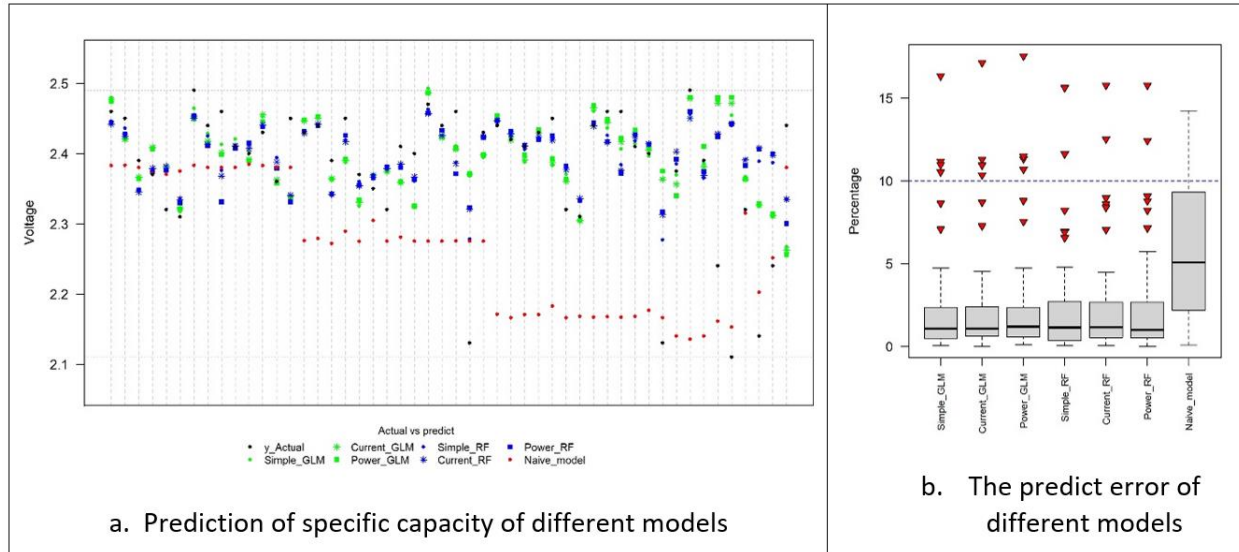


Figure 13. Voltage prediction scatter plot and the boxplot of predict absolute errors of different models

We studied the relationship between input parameters and the specific capacity and voltage using GLM, RF, and naïve model approaches. The predictions of RF models have a better performance than other models for specific capacity. The predictions of voltage from RF and GLM models are comparable but are better than naïve models.

Model accuracy

Figure 14 shows the optimized training and testing accuracies of the RF models. In this work, the model depths are from 2 to 20, the minimum sample leaf of the trees is 2 to 4, and the number of trees is 5, 10, 20, and 50. The optimized training accuracies are greater than 0.92 and less than 0.97. The testing accuracies of specific capacity RF models (see Figure 14 a) are around 0.75, and the testing accuracies of voltage RF models are around 0.8 (see Figure 14 b).

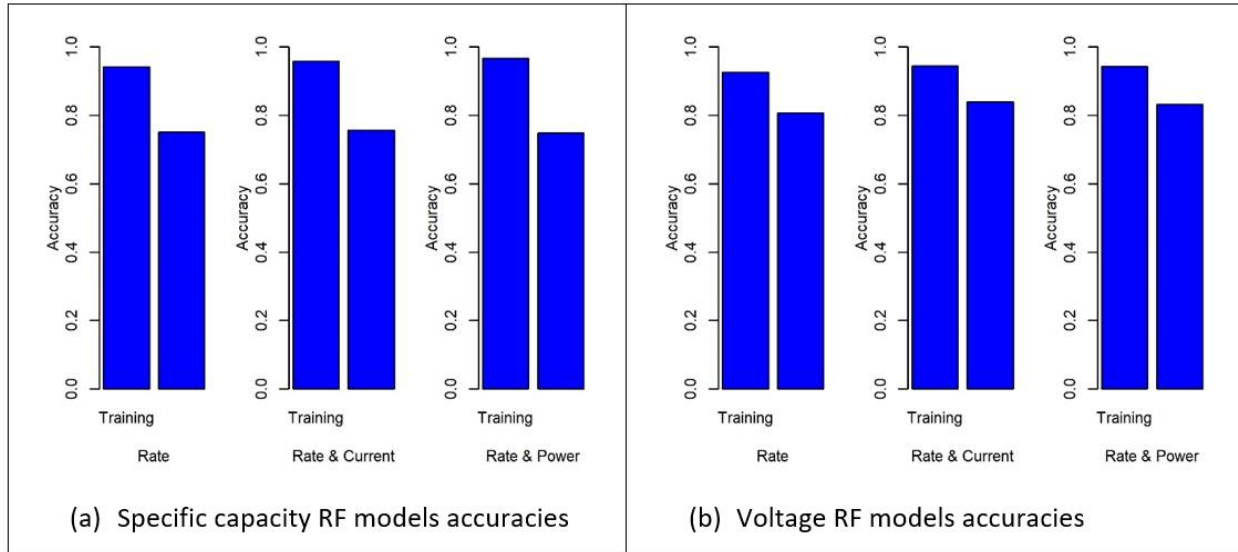


Figure 14. Training and testing accuracies of RF models.

Coding Software selection

In this work, we evaluated the RF models using the Python Scikit-learn package and the software was developed using the MATLAB. For example, Figure 15 shows the actual voltage and the mean of predictions under different conditions. The forecast represents 1-time result. The lower boundary of the actual values can be covered but can't reach the upper boundary by the 1-time results. The Pred_3T_means represents the mean of predictions of 3-time results. Both the upper boundary and the low boundary of the actual values are covered. The average of forecasts of 40-time results is not significantly different from that of 3-time results. Thus, the RF models will run three times to get comprehensive results.

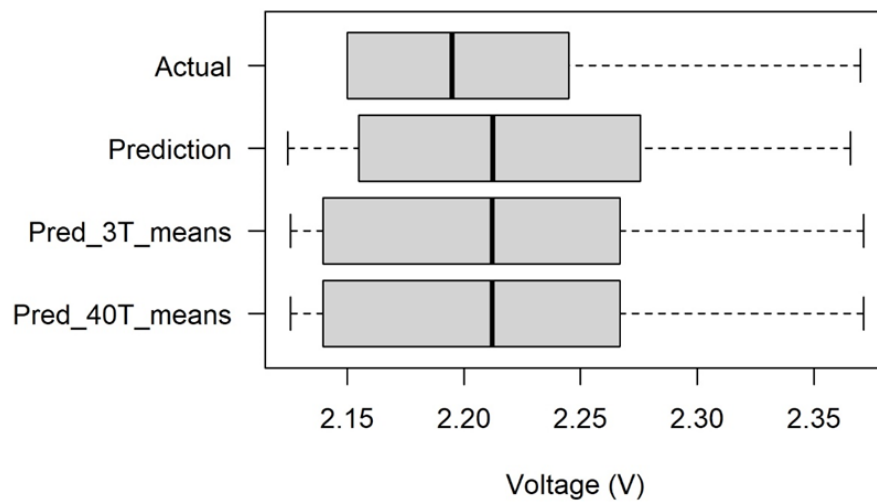


Figure 15. The actual voltage, prediction of running model 1 time, mean of predictions of running model 3 times, mean of predictions of running model 40 times of voltage model which uses the rate and physical parameters as explanatory variables.

In summary, the individual RF models are developed. The RF models will run 3 times and provide the mean of multiple times predictions to get the comprehensive results. In further work, more data needs to be collected.

- (1) Clustering analysis can be used to study the battery under different conditions.
- (2) More data help to improve the random forest models' accuracy.

2.1.3. Software development and verification

Final software

With the cell design information in section 2.1.1 and machine learning study on key parameters in section 2.1.2. The final software developed in MATLAB is achieved. Fig.16 shows the interface of the software. The full software can be obtained by contacting the PIs of this project.

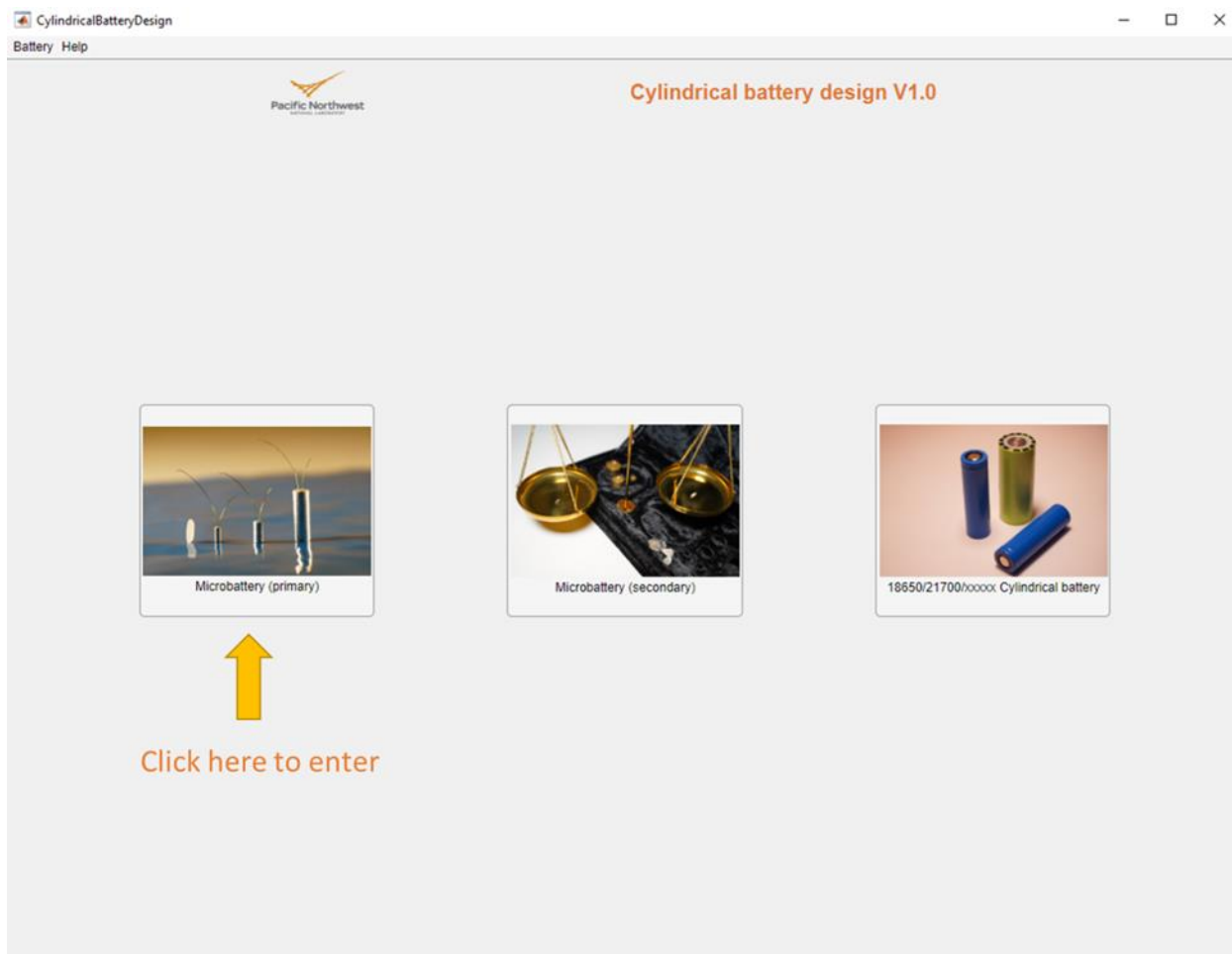


Figure 16. The interface of the cylindrical battery design app. Click first image to log in the interface for primary micro battery design.

Fig.17 shows the interface after logging into the primary micro battery design app. The main components include:

1. Battery requirement panel: Input size, current or power of the battery.
2. Design information panel: Select mode for cell design: Designed by software and Designed by user. Designed by software is integrated with machine learning model. With this mode, the materials are fixed, Carbon monofluoride(CFx) will be the cathode material while Lithium metal as anode material. No extra parameters are required by user other than following the instruction. The machine learning has slow mode and fast mode. Fast mode output the results fast (1-15 min per input parameters) but has a slightly lower accuracy as just one machine learning model is implanted. Fast mode allows the user to quickly look at the performance of the battery as designed. If the design parameters are used to produce micro battery, slow mode (3-50 min per input parameters) is recommended. Design by user allows user to build user's own battery. User will be required to input most of the parameters with this mode.
3. Command panel: Execute the order of user.
4. Image panel: Display the images of the relationship between rate/capacity with electrode parameters. Display the weight distribution of as-designed battery.
5. Estimated performance panel: Output the estimated performance of as-designed battery, including capacity, weight, and energy density.

Fig.18 and 19 are the capacity distribution, cell design, estimated performance and weight distribution of a specific input by user in the software. More detail with the software can be found in right PDF document attached behind Fig.19.

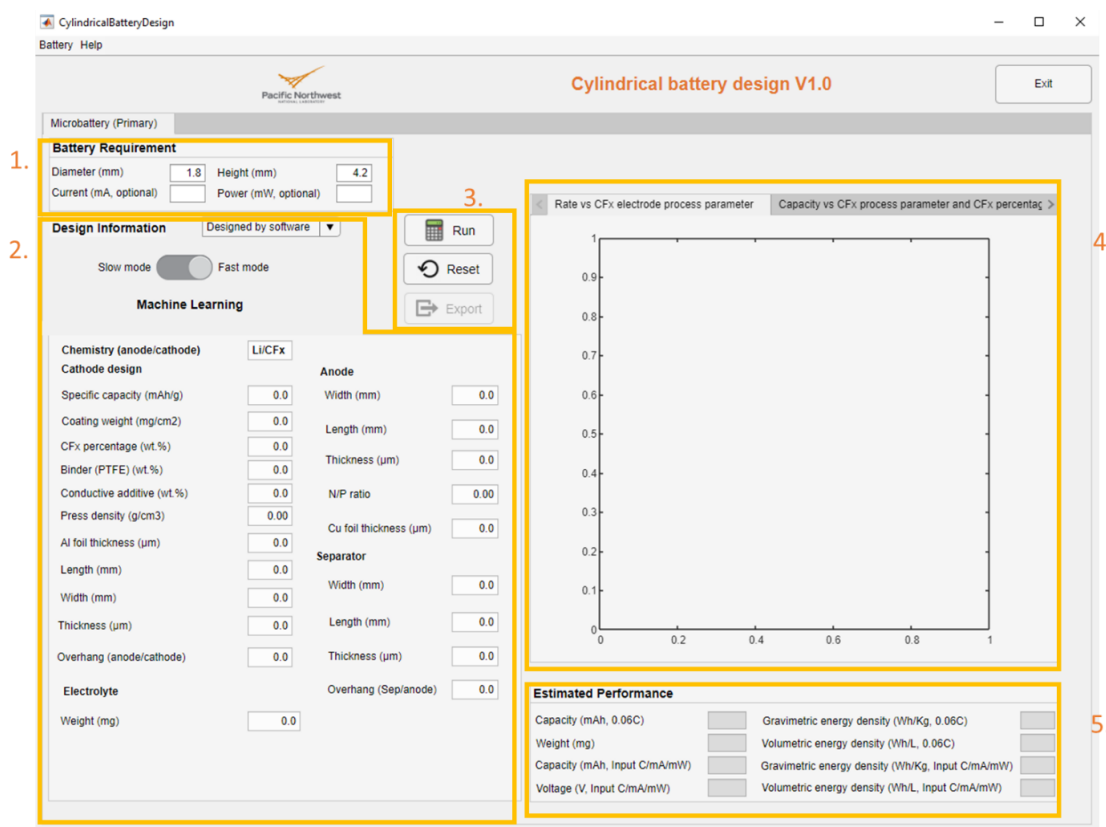


Figure 17. The interface for primary micro battery design.

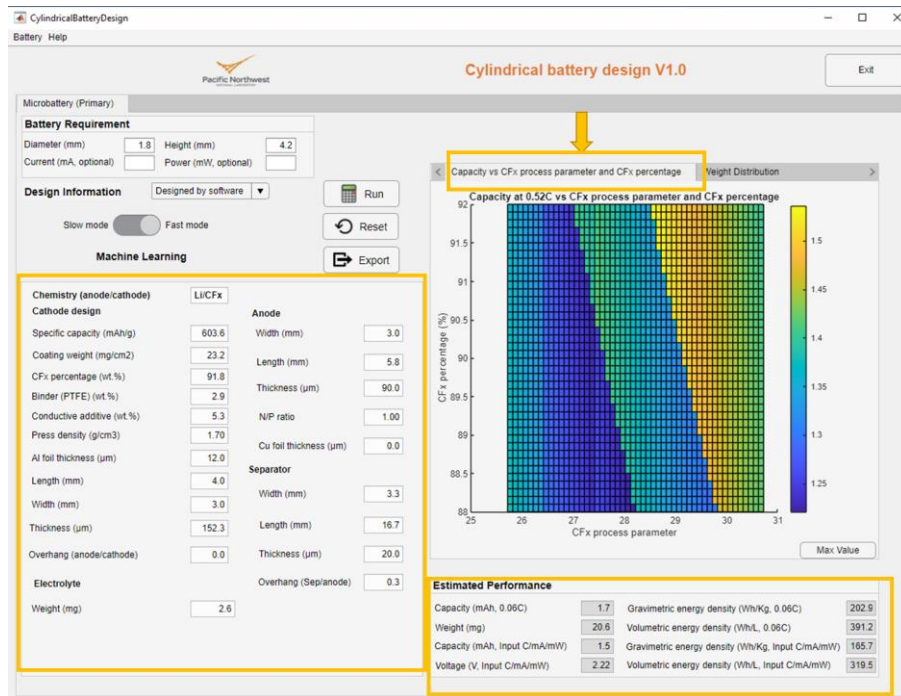


Figure 18. The capacity distribution, cell design detail and estimated performance in primary micro battery design app.

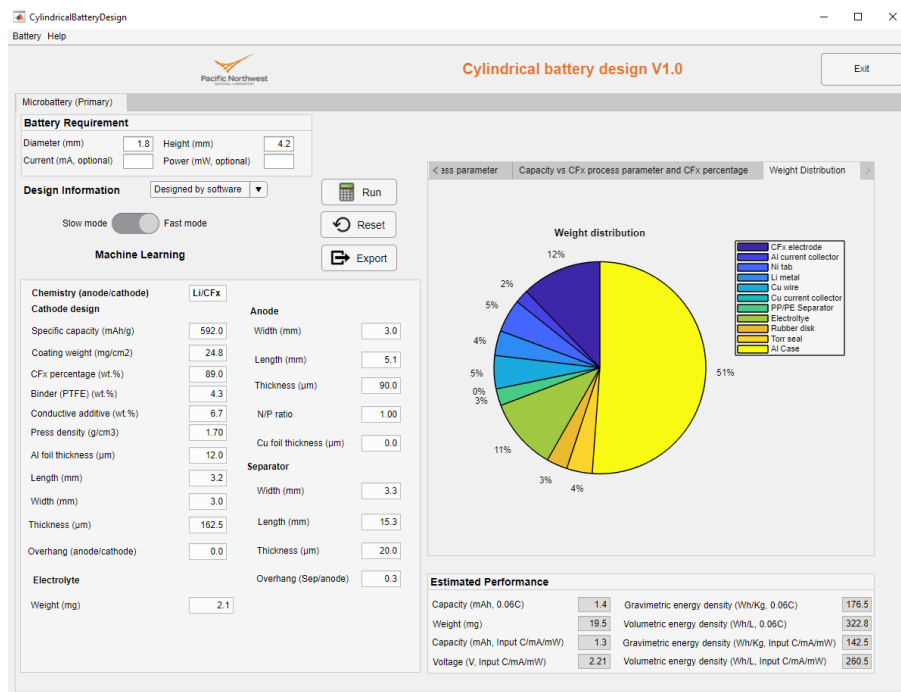


Figure 19. Weight distribution in primary micro battery design app.



Software manual-microbattery

Software verification with battery test

1st battery evaluation without ML incorporated in software

Table 3. The electrode parameters and estimated performance of six types of micro batteries with random input by user.

Random input by user			Software calculated							
Cell size	Current	Power	rate	CFx electrode			Estimated performance			
				CFx coating weight (mg/cm ²)	CFx percentage (%)	Press density (mg/cm ³)	Capacity (mAh)	Voltage (V)	Energy density (Wh/Kg)	Weight(mg)
MB1452	not provide click 0.58C		High	19.4	92	1.65	0.8	2.16	101	16.9
MB2760	5mA		High	19.1	92	1.65	4.8	2.15	186.2	55.5
MB3040		2mW	low	33.8	91.5	1.75	5.4	2.36	283.6	44.6
MB3020	not provide click 0.4C		medium	26.8	94	1.7	1.7	2.2	152.9	25
MB4750	6mA (shows rate conflict. Then use 6 mA only)	30 mW	medium	29.9	92	1.7	15.1	2.15	250	129.1
MB47100	not provide click 0.03C		ultra low	46.4	94	1.8	62.6	2.39	548.7	272.6

Table 3 shows the specific parameters given by software and estimated performance. No ML method is applied, and the method is so-called naïve mode (linear equation) mentioned above. Fig.20 are the six types of micro batteries produced according to the design information listed in Table 3. Four micro batteries for each size have been produced and tested with the testing condition listed in Table 4. As manual cell production, the actual CFx coating weight can't match the designed information provided in Table 3 well and may contribute to the accuracy of the performance prediction. With error analysis in Table 4, it can be seen that both the error of the voltage and weight prediction are ±9%. But the error of the capacity prediction in some cases is ±24%. This greatly affects the prediction of energy density which increases the error to ±38% in some cases, e.g., the extreme short type MB3020. The accuracy of the capacity prediction by software is still required to be improved next, especially for the short type of micro battery. Less than 10% of the error is the target for performance estimation. Next, we will utilize the ML model to improve the accuracy.

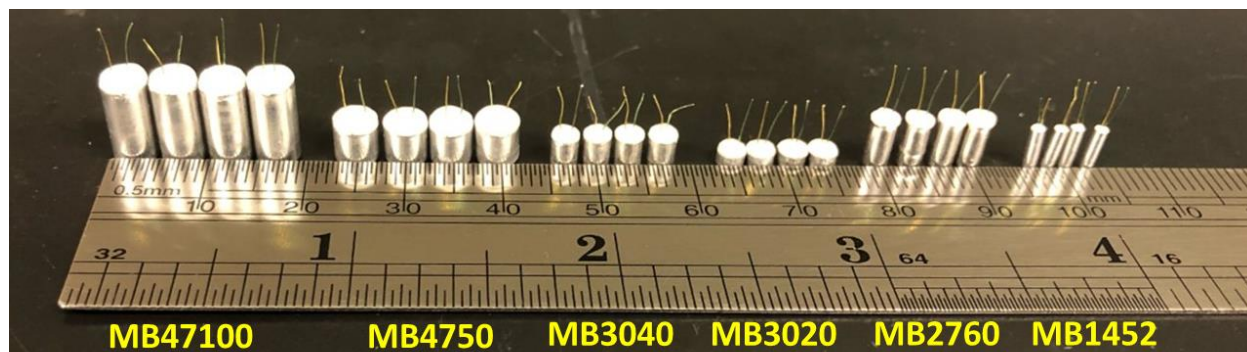


Fig.20 Six types of micro batteries produced with the design information in Table 3.

Table 4. The test results and error analysis of six types of micro batteries produced in Fig.20.

Input by user		Battery test*						
Cell size	Testing condition (calculated from last table)	Prepared CFx electrode			Achieved performance			
		CFx coating weight (mg/cm ²)	CFx percentage (%)	Press density (mg/cm ³)	Capacity (mAh)	Voltage (V)	Energy density (Wh/Kg)	Weight(mg)
MB1452	0.64 mA	20.7 (+6.7%)	92	1.74	0.99 (+23.7%)	2.24 (+3.7%)	139.2 (+37.8%)	15.9 (-5.9%)
MB2760	5 mA	22.2 (+16.7%)	92	1.58	4.6 (-4.2%)	2.11 (-1.9%)	163.9 (-12.0%)	58.8 (+5.9%)
MB3040	2 mW	34.1 (+0.9%)	91.5	1.66	4.9 (-11.1%)	2.32 (-1.7%)	239.4 (-15.6%)	47.3 (+6.1%)
MB3020	0.92 mA	27.1 (+1.1%)	94	1.75	1.3 (-23.5%)	2.14 (-2.7%)	100 (-34.6%)	27.1(+8.4%)
MB4750	6 mA	31.7 (+6.0%)	92	1.63	17.2 (+13.9%)	2.24 (+4.2%)	289.3 (+15.7%)	133.6 (+3.5%)
MB47100	1.74 mA	48	94	1.7	52.6 (-16.0%)	2.44 (+2.1%)	492 (-10.3%)	261.7 (-4.0%)

* Red means the value can't meet the designed requirement while green means the value is over the designed requirement.

2nd battery evaluation with ML incorporated in software

After integration of ML model developed in section 2.1.2, another five micro batteries with different sizes are fabricated to evaluate the software accuracy. Table 5 shows the specific parameters given by software and estimated performance with ML method applied. Fig.21 shows the five types of micro batteries produced according to the design information listed in Table 5. Two micro batteries for each size have been produced and tested with the testing condition listed in Table 5. In Fig.22, it can be seen that both the error of the capacity and voltage predictions are around ±10%. The error of the capacity prediction is improved with applied ML method. The weight error is around ± 5-10%. The error may increase with manual sealing of the battery with Torr seal. The error may be improved with better quality control in manual production and Machine learning algorithm with larger data size and distribution.

Table 5. The electrode parameters and estimated performance of five types of micro batteries with random input by user.

Random input by user				Software calculated						
Cell size	Current	Power	rate	CFx electrode			Estimated performance			
				CFx coating weight (mg/cm ²)	CFx percentage (%)	Press density (mg/cm ³)	Capacity (mAh)	Voltage (V)	Energy density (Wh/Kg)	Weight(mg)
MB1452	not provide click 0.7C		High	19.5	91.9	1.7	0.7	2.13	92.3	16.9
MB2760		5 mW	Medium	31.4	94	1.7	6.8	2.28	273.2	56.7
MB3033	0.6 mA		low	30.4	94	1.8	3.5	2.28	219.3	36.3
MB37220	30 mA	145 mW	medium	27.8	88.2	1.7	62.1	2.22	364.3	378.7
MB47100	not provide click 0.03C		ultra low	38.7	92	1.8	55.5	2.36	473.8	275.9

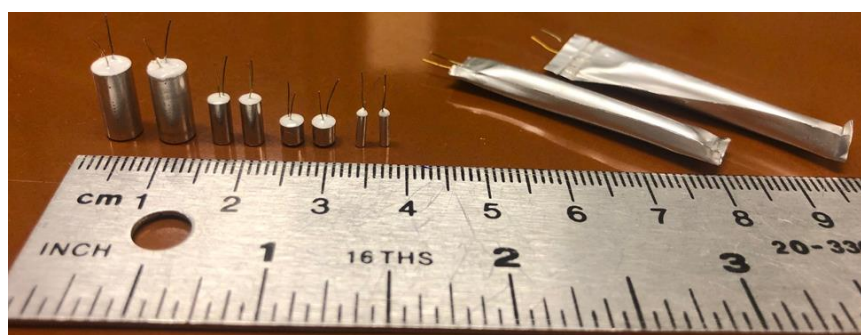


Fig.21 Five types of micro batteries produced with the design information in Table 5. The MB37220 has a little issue with the short case so the cylindrical battery is sealed in Al plastic foil.

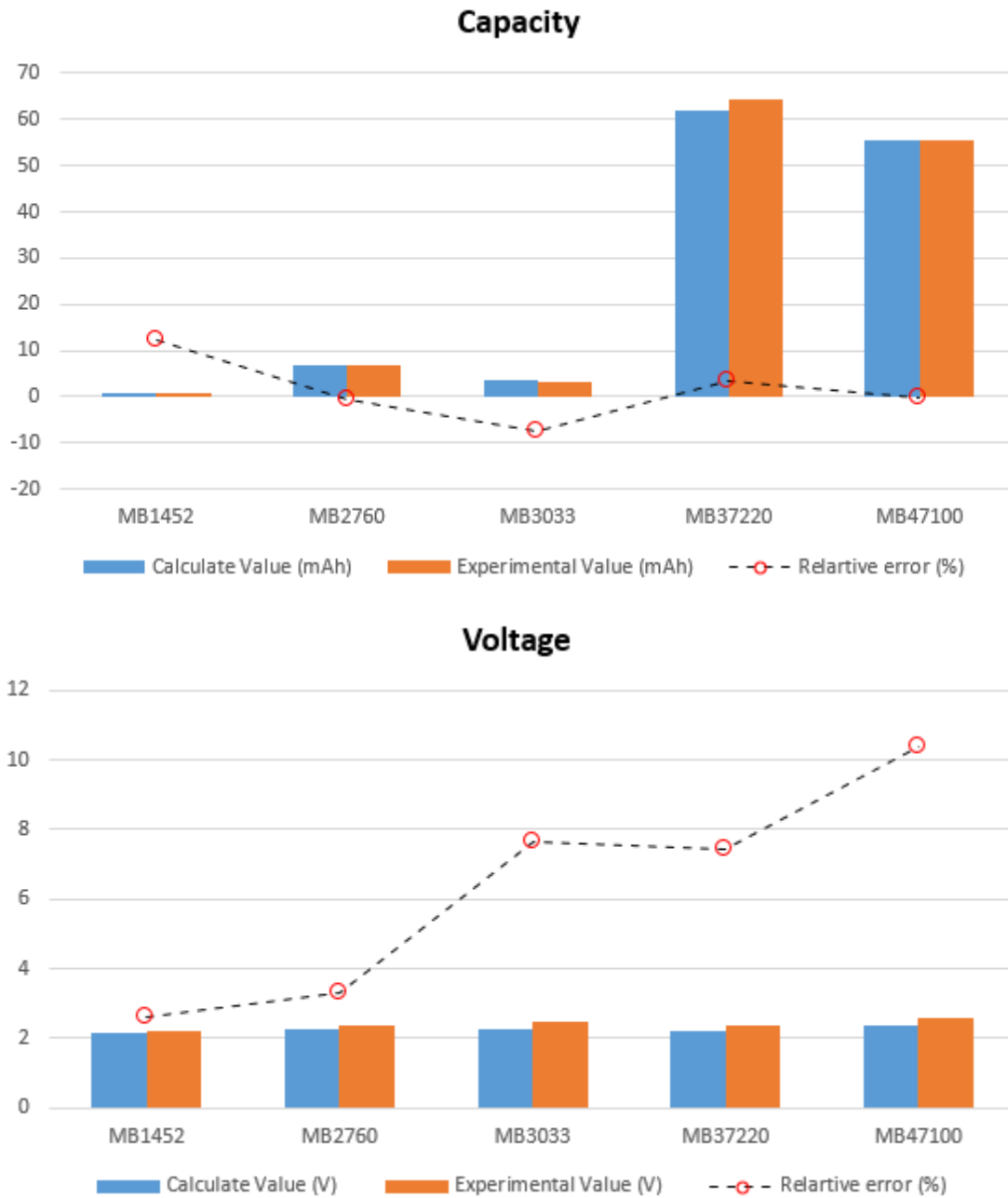


Fig.22 The experimental results and relative error of capacity and voltage with five batteries provided by software. The unit of y-axis includes both capacity (mAh, top) or voltage (V, bottom) and relative error (%). Experimental data is averaged with two cells.

2.2 Software development for cylindrical 18650/21700/xxxxx lithium-ion battery

2.2.1. Cell disassembly and data collected with commercial cylindrical LIBs

Due to the tremendous demand for improved energy storage devices for electrical vehicle and grid-level applications in the market, scientists and engineers have put much effort in making good cylindrical LIBs starting from the materials, electrodes, cell and final assembled battery pack. At PNNL, developing materials for various battery technologies is the focus. However, besides this, there is also a need to know how to design a cylindrical battery so that the laboratory can better serve the internal and external projects requiring a battery with this format. Disassembly of commercial cylindrical LIBs is a fast and cost-effective way to learn how to design a cylindrical battery. The 18650/21700 numbering system represents the dimensions of the cylindrical format. The first two digits i.e., 18 or 21, represent for the diameter of the cylindrical battery in mm, while the third and fourth digits i.e., 65 or 70 represent the height in mm. The final digits i.e., 0 indicates it is a cylindrically shaped cell. The cell design of 18650/21700 cylindrical LIBs are more complicated than micro batteries. The electrodes are bigger and double side coated. The N/P ratio varies in each cell unit due to the curvature of the JR. To balance the N/P ratio from the center of the JR to housing, the coating weight of the cathode or anode varies. Also, there are some single-side coated areas at the beginning and end of the electrodes, increasing the complexity. The number of the tabs would affect the resistance of the batteries, especially for large cylindrical batteries like 46800, determining the rate performance and heat generation. Here, we didn't do resistance design.

To achieve the required data to develop the cell design app, the commercial 18650/21700 are purchased, disassembled and measured to produce the data set, including the coating weight, electrode size, pressing density, jellyroll dimension, separator size and tab position. The cell performance can be achieved from the vendor. Table 6 shows the commercial 18650/21700 cylindrical lithium-ion batteries purchased in this project. It contains both energy type and power type batteries from different chemistries and vendors.

Table 6 Interested commercial cylindrical LIBs in this project.

18650	Vendor	Model	Chemistry	Datasheet	Link	Available	14-May		
High Power	Samsung	2.0 Ah(30A)	20S	INR	OneDrive - PNNL	https://www.batteryjunction.com/samsung-20s-inr-18650-30	v	20s	
		2.5 Ah(20A)	25S	INR	https://pnnl-my.sharepoint.com/:document/g?d=18650-p/samsung-25s-h	https://www.18650battery.com/18650-p/samsung-25s-h	v	25R	
		3 Ah(15A)	30Q	INR	https://pnnl-my.sharepoint.com/:document/g?d=18650-p/samsung-18650-p/sams	https://www.18650battery.com/Samsung-18650-p/sams	v	30Q	
	LG	3.0Ah(20A)	HG2	INR	https://pnnl-my.sharepoint.com/:document/g?d=18650-hg2	https://www.batteryjunction.com/lg-hg2-18650.html	v	HG2	
		3.0 Ah(30A)	HG6	INR	https://pnnl-my.sharepoint.com/:document/g?d=18650-li-ion-bat	https://www.batteryjunction.com/lg-hg6-inr-20650-li-ion-bat	v	HG6	
		2.5 Ah(20A)	HE4	INR	https://pnnl-my.sharepoint.com/:document/g?d=18650-he4	https://www.batteryjunction.com/lg-he4-18650.html	v	HE4	
	Sony	2.1 Ah(30A)	VTC 4	IMR	OneDrive - PNNL	https://www.18650battery.com/collections/sony-murate	v	VTC4	
		2.6Ah (30A)	VTC5	IMR	OneDrive - PNNL	https://www.batteryjunction.com/sony-vtc5-18650-2600-flat	v	VTC5D	
		2.5 Ah(35A)	VTC5a	IMR	OneDrive - PNNL	Documents\Proposal\I3T LDRD machining learning cylinder bat	https://www.wholesurgical.co	v	VTC5a
		3.0 Ah(30A)	VTC6	IMR	OneDrive - PNNL	https://www.batteryjunction.com/sony-vtc6-18650-3000-flat	v	VTC6	
		3.5 Ah (8A)	VC7	IMR	OneDrive - PNNL	https://voltaplex.com/sony-vc7-18650-battery-us18650vc7	v	x	
		3.1 Ah(6.2A)	A	NCR	OneDrive - PNNL	https://www.18650battery.com/Panasonic-18650-p/pan	v	A	
	High Energy	Panasonic	3.45 Ah (10A)	GA	NCR	OneDrive - PNNL	https://www.18650battery.com/Sanyo-18650-p/sanyo-n	v	GA
			3.55 Ah (8A)	G	NCR	https://pnnl-my.sharepoint.com/:document/g?d=18650g-3550me	https://www.imrbatteries.com/panasonic-ncr18650g-3550me	v	BD
			3.4 Ah(4.9A)	B	NCR	OneDrive - PNNL	https://www.18650battery.com/Panasonic-18650-p/pan	v	BF
Samsung		2.8 Ah(10A)	29E	INR	https://pnnl-my.sharepoint.com/:document/g?d=18650-battery	https://www.18650battery.com/Samsung-18650-Battery-	v	36G	
		3.2 Ah(10A)	32E	INR	https://pnnl-my.sharepoint.com/:document/g?d=18650-32e	https://voltaplex.com/samsung-32e-18650-battery-inr18650-32e	v	32E	
		3.5 Ah(10A)	35E	INR	https://pnnl-my.sharepoint.com/:document/g?d=18650-flat	https://www.batteryjunction.com/samsung-35e-18650-flat.ht	v	35E	
		2.8 Ah(10A)	MG1	INR	https://pnnl-my.sharepoint.com/:document/g?d=18650mg1	https://voltaplex.com/lg-mg1-18650-battery-ig18650mg1	v	MH1	
		3.2 Ah(10A)	MH1	INR	https://pnnl-my.sharepoint.com/personal/bingbin_wu_pnnl_gov/Documents/Do	https://pnnl-my.sharepoint.com/personal/bingbin_wu_pnnl_gov/Documents/Do	x		
		3.5 Ah(10A)	MJ1	INR	https://pnnl-my.sharepoint.com/personal/bingbin_wu_pnnl_gov/Documents/Docu	Documents/Proposal/I3T%20LDRD	x	MJ1	
		2.6Ah(5.2A)	26J	ICR	OneDrive - PNNL	https://www.batteryjunction.com/samsung-26j-button.html	v	M26	
Others	LG	2.5Ah(20AA)	HE2	ICR	OneDrive - PNNL	https://rechargeablepowerenergy.com/collections/battery-ce	v	29E, 2.8A	
	A123	1.1(30A)	M1B	IFR	https://pnnl-my.sharepoint.com/:document/g?d=18650-system-nanophosphate	https://www.batteryspace.com/A123-System-Nanophosphate-	v	30B, 3.0Ah	
	AA Portab	1.5Ah(5A)	EC	IFR	https://pnnl-my.sharepoint.com/:document/g?d=18650-rechargeable-g	https://www.batteryspace.com/liifeo4-18650-rechargeable-g	v	HE2	
21700	Vendor	Model	Chemistry	Datasheet	Link	Available	14-May		
20700	Samsung	3.0Ah(35A)	30T	INR	https://pnnl-my.sharepoint.com/:document/g?d=18650-30t	https://www.imrbatteries.com/samsung-30t-21700-3000mah	v	3-Aug	
	Samsung	4.0Ah(35A)	40T	INR	https://pnnl-my.sharepoint.com/:document/g?d=18650-40t	https://www.imrbatteries.com/samsung-40t-21700-4000mah	v	3-Aug	
	Samsung	5.0Ah(9.8A)	50E	INR	https://pnnl-my.sharepoint.com/:document/g?d=18650-50e	https://www.imrbatteries.com/samsung-50e-21700-5000mah	v	3-Aug	
	Tesla	5Ah (10A)	model3	NCR	https://pnnl-my.sharepoint.com/:document/g?d=18650-tesla	https://www.techdirectclub.com/21700-lithium-ion-battery-1	v	3-Aug	
					http://eleteks-com.sell.everychina.com/p-108442467-panaso				
			IMR	Lithium manganese oxide(LiMn2O4)			Sanyo NCR		
			INR	Lithium nickel cobalt manganese oxide(LiNiMnCoO2)					
			NCR	Lithium nickel cobalt aluminum oxide (LiNiCoAlO2)					
			ICR	Lithium cobalt oxide (LiCoO2)					
			IFR/LFP	Lithium iron phosphate(LiFePO4)					
Battery charger:					https://www.18650battery.com/collections/18650-battery-charger/products/skyrc-mc3000	X2	v		

Prior to purchasing the commercial lithium-ion batteries, a SOP relating to the safe disassembly of discharged LIB must be developed. This SOP describes the standard operation of disassembly of the discharged commercial 18650/21700 cylindrical LIBs in the PSL facility. The term “discharged” means the cylindrical LIB is fully discharged to its lower limit voltage and the state of charge (SoC) is 0%. The lower limit voltage is the discharge cut-off voltage provided by the vendor, typically 2.5 V. The disassembly of cylindrical cells above 0% SoC is out of the scope of this SOP. Other two cell formats i.e., prismatic type and pouch type LIBs, are also out of the scope of this SOP.

As showed in Fig.23, discharge the battery to lower limit voltage in an N₂-filled environment chamber. Then the discharged battery can be transferred to an Ar-filled glove box for disassembly. The typical disassembly procedure includes checking the safety toolbox is ready (Fig.24). Remove the plastic cover on the battery. Use the pipe cutter to cut the position of the “crimped can” on the battery. Cut the positive tab off with a ceramic scissor. Insulate the positive tab on top of the Jellyroll with tape. Carefully cut and peel off the can with a nipper. Collect the battery can in one container as it produces sharp edge. Unroll the jellyroll carefully and separate the cathode and anode sheets one by one. An IR camera held by the second staff is required during the whole disassembly process. The full process can be found in following pdf document.



SOP Disassembly of discharged commerci

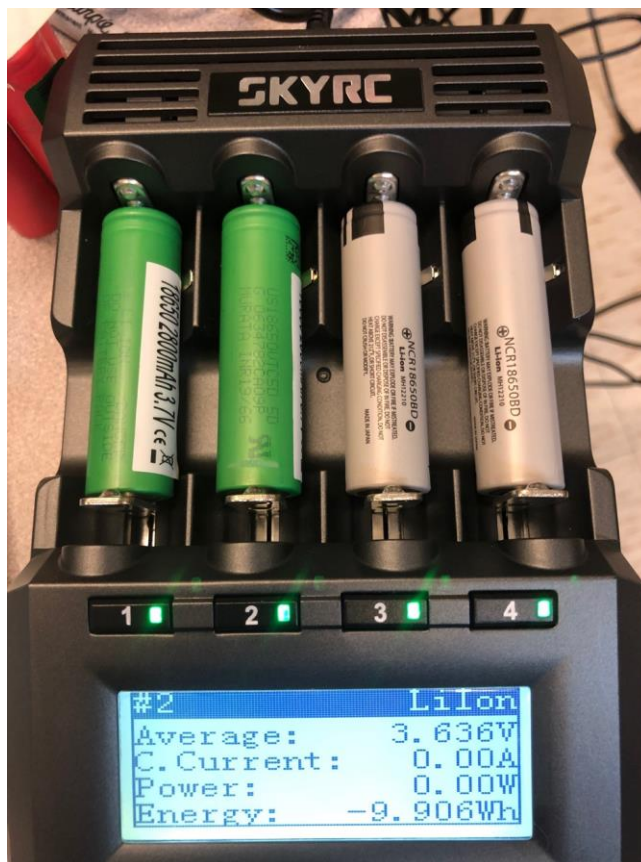


Fig.23 Device to discharge the cylindrical batteries.



Fig.24 Setup for cell disassembly of commercial 18650/21700 LIBs at PSL 522A.

With approved SOP of cell disassembly, the detailed parameters related to the commercial cylindrical LIBs can be obtained. Table 7 shows part of the datasheet collected from a disassembled commercial battery. The detailed data can be found in the excel attached after the table. Finally, this data can be used to create the original design sheet for cylindrical lithium-ion battery (Table 8).

Table 7 Data collection of disassembled commercial cylindrical LIBs.

Sample #	31-1		
Date			
Battery info	LG MJ1	Brand/model	
Rated capacity	3500	mAh	
Rated voltage	3.635	V	
Rated current	10	A	
Cell 1	For size, capacity, characterization		
discharge capacity		mAh	
resistance		mΩ	
energy	12.7225	Wh	
Battery total we	46.841	g containing plastic cover	
	46.473	g no plastic cover	
1. Remove case			
JR structure			
Diameter:	17.84	mm	Top
Height:	60.7	mm	Back
Tab position:			End
(describe, mark on picture			End
End layer:	Sep	(Al, Cu, Separator?)	
Tape	clear	color and position	
Tape size	30.6425	L*W*T	cm2
Center pore D	2.95	mm	
Comments:	central pin	g	Case thickness 0.12 mm
		Odmm*Idmm*Hmm	bottom thickness 0.31 mm
insulate pats			
Top cap			
2. Unroll JR			
End position	7	mm	C/A
	8	mm	S/A



%2331%20LG%20MJ
1%2018650%20Parai

Table 8 Design sheet of 18650/21700 cylindrical LIBs.

		Cylindrical battery design V1.0		18650/21700 cylindrical battery		Pacific Northwest NATIONAL LABORATORY		
Battery requirements								
Diameter (mm)	18	Height (mm)	65					
Working voltage (V)	3.6							
Estimated performance						Visuable interface		
Capacity (mAh)	1264	Energy (mWh)	4.55			Show J/R structure and electrodes design, NP ratio design, J/R size control, weight distribution		
Energy density (Wh/l)	95.9	Weight (g)	47.5					
Design informati		Designed by user						
Chemistry (anode/cath)	Graphite/4.1V NMC111							
Cathode	1st discharge specific capacity (mAh/g)	109.0	Anode	1st charge specific capacity	330.0			
	1st CE (%)	96.0		1st CE (%)	92.0			
	Coating weight (mg/cm ² , sideA, insic)	14.5		NP ratio (total)	1.1			
	Coating weight (mg/cm ² , sideB, outsi)	15.1		Coating weight (mg/cm ² , sic)	5.5			
	A/B coating weight ratio (%)	96.0		Coating weight (mg/cm ² , sic)	5.5			
	Active material ratio(wt.%)	94.0		A/B coating weight ratio (%)	100			
	Binder ratio (wt.%)	2.0		Active material ratio(wt.%)	94.5			
	Carbon ratio (wt.%)	4.0		Binder ratio (wt.%)	3.5			
	Press density (g/cm ³)	2.8		Carbon ratio (wt.%)	2.0			
	Current collector thickness (µm)	25.0		Press density (g/cm ³)	1.4			
	Current collector density (g/cm ³)	2.7		Current collector thickness (µm)	15.0			
Length	C1(mm, sideA)	702		Current collector density (g/cm ³)	8.9			
	C2(mm, sideB)	760.0		Overhang (anode/cathode,w	1.5			
	C3(mm, front to sideB)	50.0	Length	A1(mm, sideA)	772.0			
	C4(mm, sideA to sideB)	12.0		A2(mm, sideB)	772.0			
	C5(mm, front to tab)	5.0		A3(mm, end to sideA)	75.0			
	C6(mm, end to sideA)	70.0		A4(mm, sideB to tab)	5.0			
	C7(mm, end to sideB)	15.0		Total length (mm, with CC)	847.0			
	Total length (mm, with CC)	825.0		Overhang (anode/cathode,le	12.0			
	Width (mm)	57.0		Width (mm)	58.5			
	Total thickness (µm)	130.7		Total thickness (µm)	92.5			
	Average areal capacity (mAh/cm ²)	1.5		Average areal capacity (mAh/cm ²)	1.7			
	Total weight (g)	15.5		Total weight (g)	17.08			
Separator	Width (mm)	60.5	Wind pin	Diameter (mm)	3.5			
	Length (mm)	1734.0	Tabs	Weight (g, cathode side)	1.0			
	Thickness (µm)	20.0		Weight (g, anode side)	1.0			
	Overhang (Sep/anode, total)	2.0	Can	Weight (g)	9.3			
	Density (g/cm ³)	1.0		Wall thickness (mm)	0.2			
Electrolyte	Weight/capacity (g/Ah)	1.8	J/R size control	J/R diameter (mm)	17.0			
	Weight (g)	2.27		J/R area/available area in cas	90.1			

2.2.2. Software development

With the analysis of the data collected from various commercial LIBs, a software relating to large cylindrical LIBs can be developed in MATLAB. Fig. 25 shows the interface of the 18650/21700/xxxxx cylindrical batteries in the battery design app.

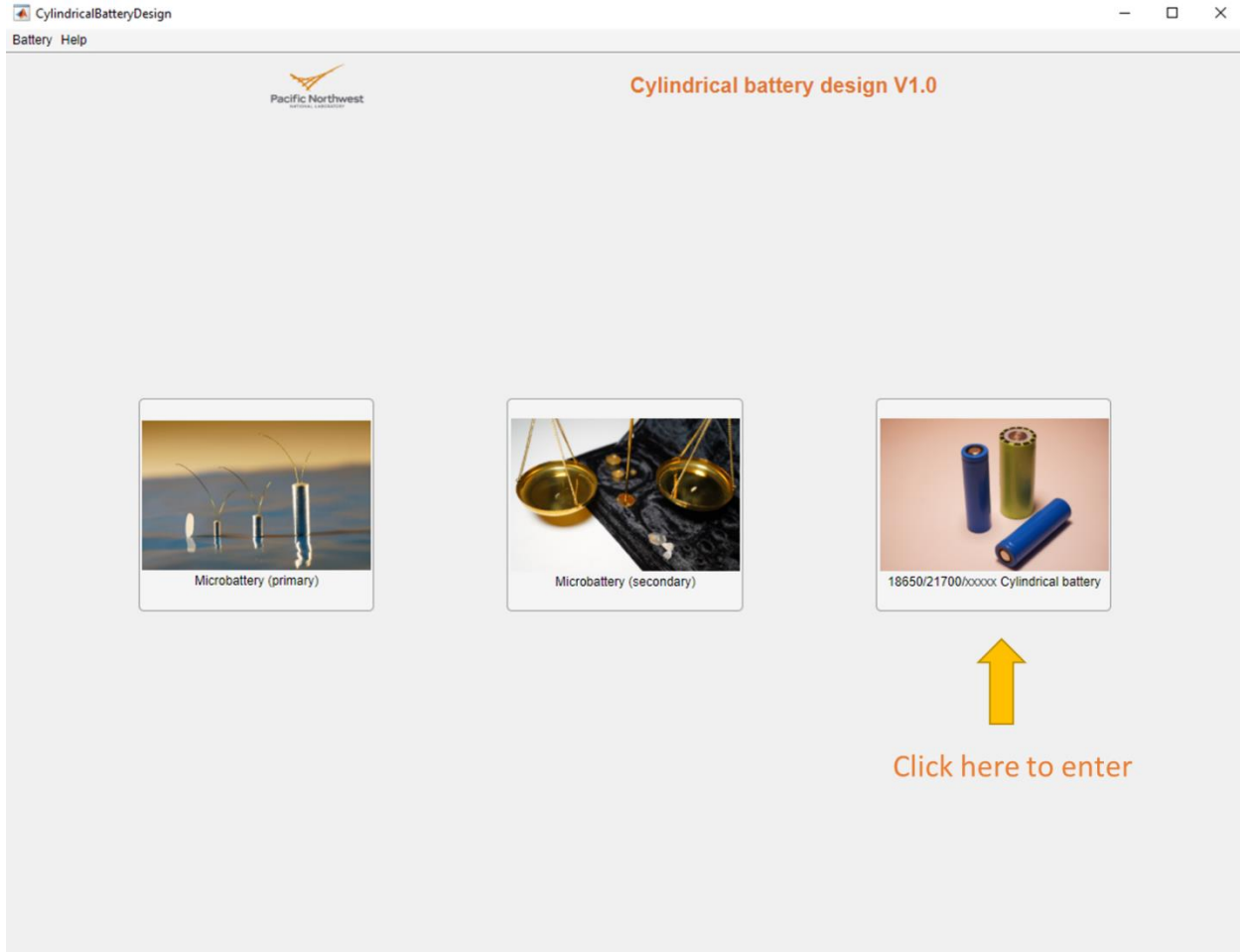


Fig.25 The interface of the cylindrical battery design app. Click second image to log in the interface for secondary micro battery design.

Fig.26 shows the interface of 18650/21700/xxxxx cylindrical battery design. The main components include:

1. Battery requirement panel: Input size and voltage of the target battery.
2. Design information panel: Input all the preferred parameters for the cathode/anode electrodes, electrolyte, separator, battery house and other components.
3. Command panel: Execute the order of user.
4. Image panel: Display the images of battery and cathode/anode electrodes. Display the images of N/P ratio and A1 range to check the qualification of a cell design input by user. Display the weight distribution of as-designed battery.
5. Estimated performance panel: Output the estimated performance of as-designed battery, including capacity, weight, energy, and energy density.

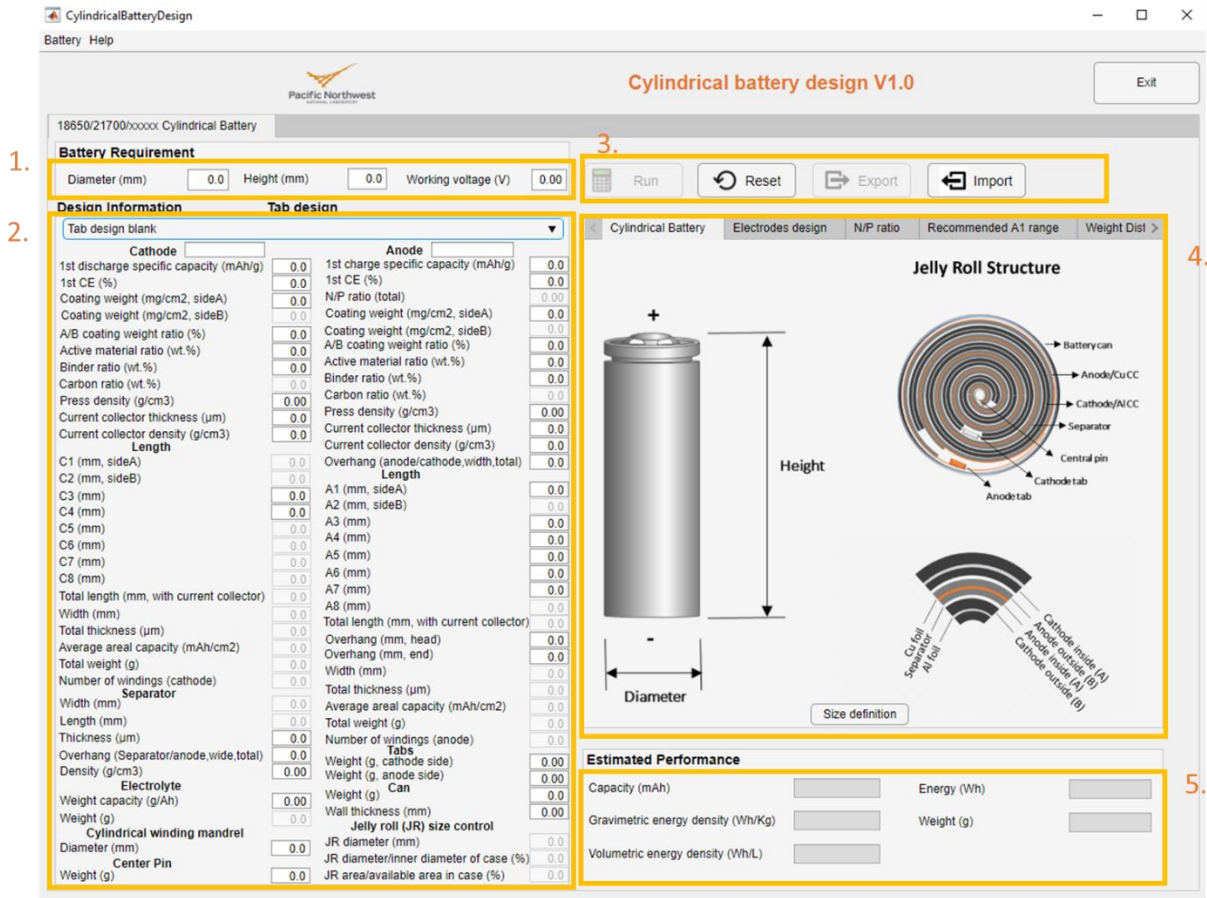


Fig.26 Interface of 18650/21700/xxxxx cell design in the software.

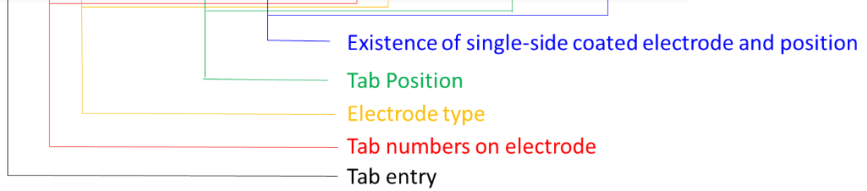
The software comprises 10 types of Tab designs learned from the commercial batteries, including energy-type batteries and power-type batteries. Tab design information is shown with a special expression. Fig. 27 shows the definition of the expression of the tab design.

A typical design process can be found in Fig.28-30, relating to the N/P ratio design, electrode size design and weight distribution of the battery with input parameters in the software. The detail design process is available in the following pdf document.



Software manual-18650 21700

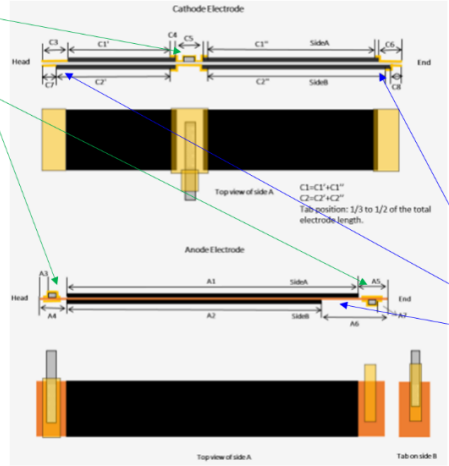
Tab8: 1-Cathode Tab (In, Single-H,E) / 2-Anode Tabs (Out-H,E, Single-E)



Tab Position:

In: Tab located in the electrode

Out-H,E,: Tabs located outside of the electrodes. H means head of the electrode while E for end. If H or/and E are presenting, it means, there is/are tab/tabs locating at head or end/ head and end of the electrodes.



Existence of single side coated electrode and position:

Single: single-side coated electrode exists.

Single-H,E,: H means head of the electrode while E for end.

If H or/and E are presenting, it means, there is/are single-side coated electrode/electrodes locating at head or end/ head and end of the electrodes.

Fig.27 Description of the tab design in the software.

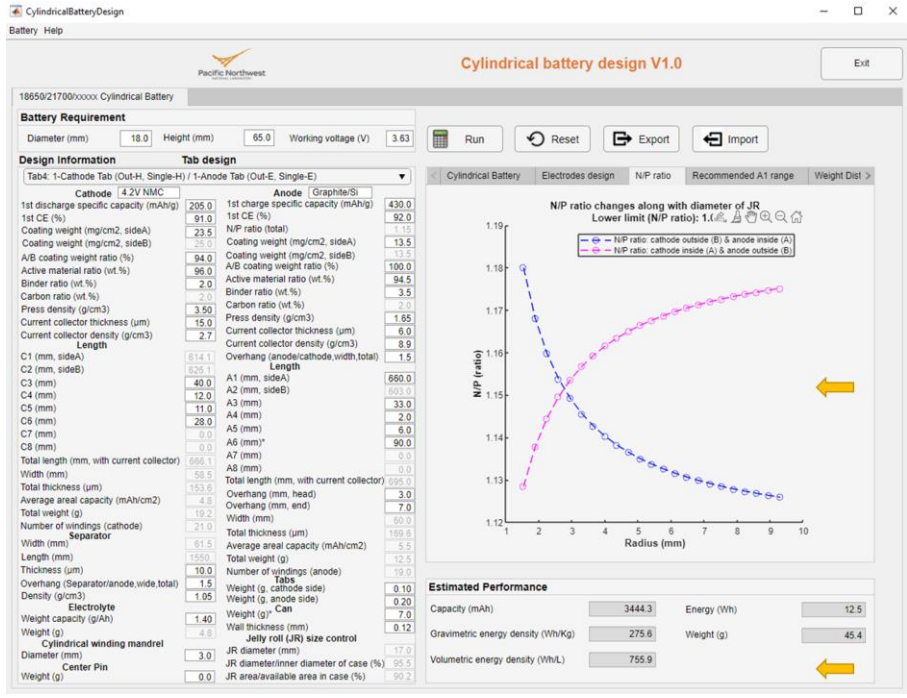


Fig.28 N/P ratio design and distribution of the battery with input parameters in the software.

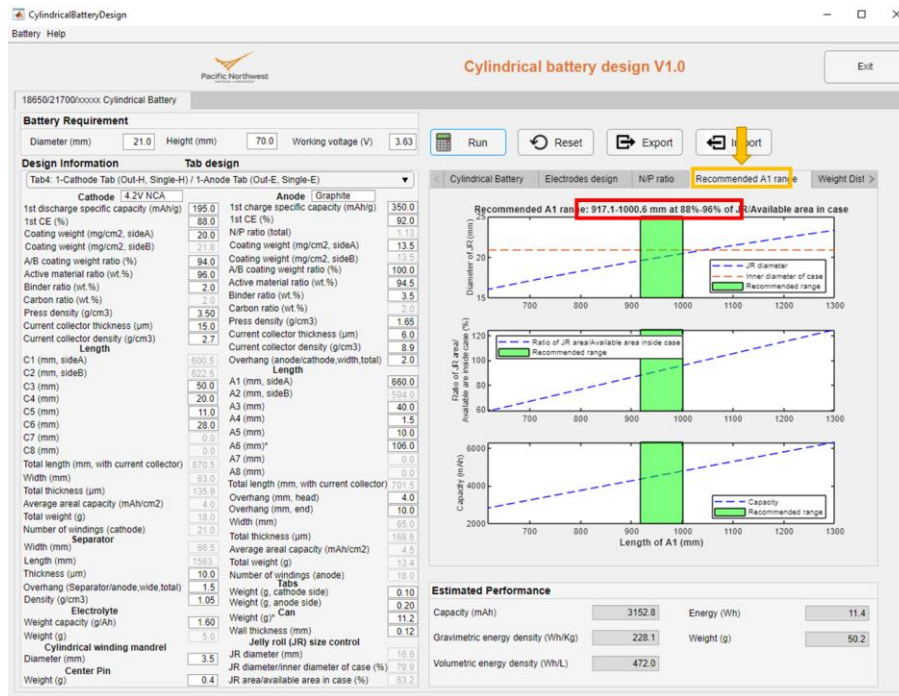


Fig.29 Electrode design and distribution of the battery with input parameters in the software.

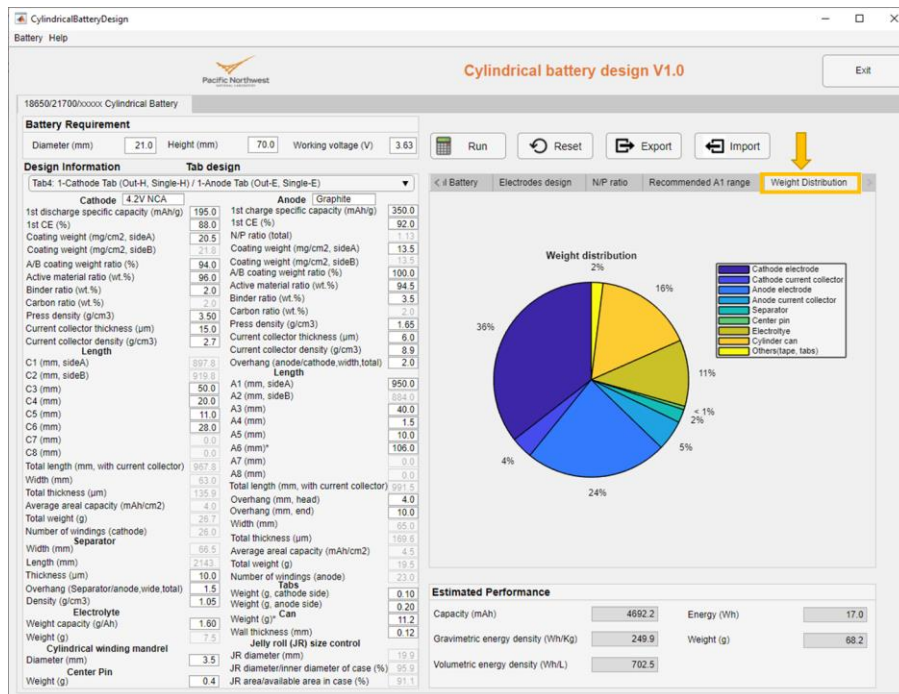


Fig.30 Weight distribution of the battery with input parameters in the software.

2.3 Summary

A software that delivers optimal design parameters and performance predictions for cylindrical cells, which can range in size from micro batteries to electric vehicle (EV) batteries, is developed in MATLAB.

1. Several hundreds of Li/CF_x primary micro batteries are produced to collect data for machine learning study on key parameters of the battery design. The software for primary micro battery with machine learning algorithm has a high accuracy on performance prediction, typical, around $\pm 10\%$ of the errors on capacity, voltage and weight estimation.
2. With approved SOP of cell disassembly, several tens of commercial 18650/21700 cylindrical LIBs are disassembled and measured to collect the information on coating weight, electrode size and jellyroll dimension. With these parameters, a software is developed to design the cylindrical LIBs with performance closed to commercial batteries.

Contact PIs for software installation and use.

3.0 References

1. Michael J. Lain, James Brandon, and Emma Kendrick. 2019. "Design Strategies for High Power vs. High Energy Lithium Ion Cells." *Batteries* 5(4): 64; <https://doi.org/10.3390/batteries5040064>
2. Jie Xiao, Yang Yang, Dianying Liu, and Zhiqun D Deng, Li-Batt Design App, Pacific Northwest National Laboratory, Richland, WA, USA
3. Chen H., S.S. Cartmell, Q. Wang, T.J. Lozano, Z. Deng, H. Li, and X. Chen, et al. 2014. "Micro-battery Development for Juvenile Salmon Acoustic Telemetry System Applications." *Scientific Reports* 4: PNNL-SA-84994. doi:10.1038/srep03790
4. Wang Y., S.S. Cartmell, Q. Li, J. Xiao, H. Li, Z. Deng, and J. Zhang. 2017. "A reliable sealing method for micro batteries." *Journal of Power Sources* 341: PNNL-SA-119837. doi:10.1016/j.jpowsour.2016.12.024

Pacific Northwest National Laboratory

902 Battelle Boulevard
P.O. Box 999
Richland, WA 99354

1-888-375-PNNL (7665)

www.pnnl.gov